

**PREPARATION OF BILIRUBIN IMPRINTED POLYMERIC  
ADSORBENTS**

**BİLİRUBİN BASKILANMIŞ POLİMERİK ADSORBENTLERİN  
HAZIRLANMASI**

**GÖZDE BAYDEMİR**

Submitted to  
HACETTEPE UNIVERSITY  
THE INSTITUTE FOR GRADUATE STUDIES  
IN SCIENCE AND ENGINEERING  
in partial fulfillment of the requirements for the degree of  
MASTER OF SCIENCE  
in  
CHEMISTRY DEPARTMENT

2006

## BİLİRUBİN BASKILANMIŞ POLİMERİK ADSORBENTLERİN HAZIRLANMASI

GÖZDE BAYDEMİR

### ÖZ

Bu çalışmanın amacı bilirubin baskılanmış polimerler hazırlayarak, hiperbilirubinemili insan plazmasından bilirubini seçici olarak uzaklaştırmaktır. Kompleksleştirici monomer olarak N-Metakroil-(L)-tirozinmetilesteri (MAT) seçilmiştir. İlk olarak, N-Metakroil-(L)-tirozinmetilesteri (MAT) ve metakroil klorür reaksiyonundan N-Metakroil-(L)-tirozin (MAT) sentezlenmiş ve nükleer manyetik rezonans (NMR) ile karakterize edilmiştir. Daha sonra bilirubin MAT ile kompleksleştirilerek bilirubin baskılanmış poli(2-hidroksietil metakrilat-N-metakroil-(L)-tirozinmetilesteri) MIP partikülleri yığın polimerizasyonu ile sentezlenmiştir. Bundan sonra, hedef molekül (bilirubin), sodium karbonat ve sodium hidroksit çözeltileri kullanılarak sökülmüştür. MIP partikülleri elemental analiz, şişme testleri, fourier transform infrared spektroskopisi (FTIR) ve taramalı elektron mikroskobu (SEM) ile karakterize edilmiştir. Bilirubin adsorpsiyon deneyleri insan plazmasından kesikli sistemde yapılmıştır. Selektivite testleri, yarışmacı ajan olarak kolesterol ve testosteron kullanılarak yapılmıştır. Elde edilen sonuçlar şu şekildedir; MIP ve baskılanmamış (NIP) partiküllerin sudaki şişme oranları sırasıyla: %64.7 ve %51.3; elemental analiz sonuçlarına göre, MIP partiküllerinin MAT içeriği 69.0 µmol/gram olarak bulunmuştur. SEM fotoğrafları yüzey porozitesi ve pürüzlülüğünü göstermektedir. Hedef molekül (bilirubin) polimer yapısından başlangıç konsantrasyonunun %87'si oranında sökülmüştür. Bilirubin adsorpsiyonu artan bilirubin konsantrasyonlarında 3.431 mg/mL'ye kadar artış göstermiştir. İnsan plazmasından maksimum bilirubin adsorpsiyon kapasitesi kuru partikül ağırlığı başına 3.4 mg/g bilirubin olarak bulunmuştur. MIP partikülleri kolesterol ve testosterona göre sırasıyla 6.3 ve 3.0 kat daha seçicidir. Bu çalışmada MIP partiküllerin tekrar kullanılabilirlikleri de incelenmiştir. MIP partiküllerinde aynı adsorbent kullanılmak koşuluyla beş adsorpsiyon-desorpsiyon döngüsü sonucu bilirubin adsorpsiyon kapasitesinde ihmal edilebilir düzeyde bir kayıp gözlenmiştir.

**Anahtar Kelimeler :** Moleküler Baskılanmış Polimerler (MIP), Bilirubin Baskılama, Metakroilamidotirozin

**Danışman :** Prof. Dr. Adil DENİZLİ, Hacettepe Üniversitesi, Kimya Bölümü, Beytepe, ANKARA

## **PREPARATION OF BILIRUBIN IMPRINTED ADSORBENTS**

### **GÖZDE BAYDEMİR**

#### **ABSTRACT**

The aim of this study is to prepare bilirubin-imprinted polymer for selective removal of bilirubin from hyperbilirubinemic human plasma. N-methacryloyl-(L)-tyrosine (MAT) was chosen as the complexing monomer. In the first step, functional monomer MAT was synthesized by the reaction of L-tyrosine methylester and methacryloyl chloride and characterized with nuclear magnetic resonance (NMR). Then, bilirubin was complexed with MAT and the bilirubin-imprinted poly(2-hydroxyethyl methacrylate-N-methacryloyl-(L)-tyrosine) (MIP) particles were produced by bulk polymerization. After that, the template molecules (i.e., bilirubin) were removed using sodium carbonate and sodium hydroxide. MIP particles were characterized by elemental analysis, swelling tests, fourier transform infrared spectroscopy (FTIR) and scanning electron microscopy (SEM). Bilirubin adsorption experiments from human plasma were performed in a batch experimental set-up. Cholesterol and testosterone were used as competing molecules in selectivity tests. Obtained results were as follows: swelling ratio of MIP and non-imprinted (NIP) particles were 64.7% and 51.3% in water. According to the elemental analysis results, incorporation of MAT was 69.0  $\mu\text{mol/g}$  for MIP particles. SEM photographs showed the surface roughness and porosity. Template molecules (i.e., bilirubin) were removed from the polymer structure in the ratio of 87% of the initial concentration. Bilirubin adsorption increased with the increase in bilirubin concentration up to 3.431 mg/mL. The maximum bilirubin adsorption capacity from human plasma was 3.4 mg/g of the dry weight of particles. MIP particles were 6.3 and 3.0 times selective with respect to the cholesterol and testosterone, respectively. Reusability of MIP particles was also investigated. MIP particles showed negligible loss in the bilirubin adsorption capacity after five adsorption-desorption cycles with the same adsorbent.

**Keywords** : Molecularly Imprinted Polymers (MIP), Bilirubin Imprinting,  
Methacryoylamidotyrosine (MAT)

**Supervisor** : Prof. Dr. Adil DENİZLİ, Hacettepe University, Chemistry,  
Beytepe, ANKARA

## ACKNOWLEDGEMENT

First and foremost, I would like to express my sincere thanks to my supervisor Prof. Dr. Adil Denizli for his continuing guidance, suggestions and encouragement throughout the research with great patience. It has been a great honour for me to work with him.

Also, I wish to express my thanks to Prof. Süleyman Patır and Assist. Prof. Dr. Abbas Taner for their kind helps and suggestions.

In addition, I would like to thank all of the Biochemistry Research Group, Dr Handan Yavuz, Dr. Sinan Akgöl, Dr. Mehmet Odabaşı, Lokman Uzun, Nilay Bereli, A.Müge Andaç, Bora Garipcan, Dr. Serpil Özkara, Melike Karataş, Nilgün Başar, Başak Şaşmaz, Veyis Karakoç, Deniz Türkmen, Ahmet Hamdi Demirçelik, Erkut Yılmaz for their help, friendship and cooperation. My M.Sc. period would not have been enjoyable without them. I can never forget their presence throughout my graduate and undergraduate education.

Especially thanks are devoted to Nilay Bereli, Dr. Handan Yavuz and A.Müge Andaç for their valuable guidance, their professional helps, understanding, support and encouragement throughout this study. I never forget the motivations and support of my invaluable friends, especially Nilay Bereli.

I would also have to add all the members of the Chemistry Department whom I needed help or advice. Everybody has been extremely nice and kind.

I would like to thank my dear friends Güngör Erseymen, Filiz Cengiz for their helps and encouragement during this study.

I extend my sincere appreciation to my family for their patience, helps, encouragement, not only throughout my academic years, but also my whole life.

And also special thanks to A.Tolga Peşint for always being with me.

## INDEX

<b>ÖZ</b> .....	<b>I</b>
<b>ACKNOWLEDGEMENT</b> .....	<b>V</b>
<b>INDEX</b> .....	<b>VI</b>
<b>FIGURE LEGEND</b> .....	<b>VIII</b>
<b>TABLE LEGEND</b> .....	<b>IX</b>
<b>1. INTRODUCTION</b> .....	<b>1</b>
<b>2. GENERAL INFORMATION</b> .....	<b>4</b>
<b>2.1. BILIRUBIN</b> .....	<b>4</b>
2.1.1. Production of Jaundice .....	5
2.1.2. Removal of Bilirubin .....	6
2.1.3. Detection of Bulirubin.....	6
2.1.4. Bilirubin as an Antioxidant.....	7
2.1.5. Bilirubin and Protein Phosphorylation.....	8
<b>2.2. HEMOPERFUSION</b> .....	<b>8</b>
<b>2.3. MOLECULAR IMPRINTING</b> .....	<b>10</b>
2.3.1. Naturally Occurring Receptors .....	10
2.3.2. Artificial Receptors.....	12
2.3.3. Receptors for Practical Applications.....	13
2.3.4. The Importance of the Molecular Imprinting Method .....	13
2.3.5. General Principle of Molecular Imprinting.....	14
2.3.6. Covalent Imprinting and Non-covalent Imprinting.....	16
2.3.7. Hybridization of Covalent Imprinting and Non-covalent Imprinting.....	20
<b>3. EXPERIMENTAL</b> .....	<b>21</b>
<b>3.1. MATERIALS</b> .....	<b>21</b>
<b>3.2. PREPARATION OF POLYMERIC PARTICLES</b> .....	<b>21</b>
3.2.1. Synthesis of N-Methacryloyl-(L)-Tyrosine .....	21
3.2.2. Preparation of Bilirubin Imprinted Poly(HEMA-MAT) Particles.....	22
3.2.3. Removal of the Template (Bilirubin) .....	22
<b>3.3. CHARACTERIZATION OF PARTICLES</b> .....	<b>23</b>
3.3.1. Swelling Test .....	23

3.3.2. Surface Morphology.....	23
3.3.3. Elemental Analysis.....	23
3.3.4. FTIR Studies.....	24
3.3.5. NMR Studies.....	24
<b>3.4. ADSORPTION-DESORPTION STUDIES.....</b>	<b>24</b>
3.4.1. Bilirubin Remaval From Human Plasma.....	24
<b>3.2 DESORPTION AND REPEATED USE.....</b>	<b>26</b>
<b>4. RESULTS AND DISCUSSION.....</b>	<b>27</b>
4.2.1. Effect of Time.....	34
4.2.2. Effect of Equilibrium Concentration of Bilirubin.....	36
4.2.3. Langmuir Adsorption Model And Adsorption Dynamics.....	37
4.2.4. Selectivity Experiments.....	43
<b>4.3. DESORPTION AND REPEATED USE.....</b>	<b>45</b>
<b>5. CONCLUSION.....</b>	<b>47</b>
<b>6. REFERENCES.....</b>	<b>49</b>

## FIGURE LEGEND

Figure 2.1. Degradation of heme to bilirubin.....	4
Figure 2.2. Main steps in bilirubin formation and metabolism. (Monoglucuronides are also formed in addition to the diglucuronide structure shown.).....	5
Figure 2.3. Intramolecular cyclization of bilirubin in presence of light to form lumirubin.....	6
Figure 2.4. Schematic illustration of molecular imprinting .....	15
Figure 2.5. Concept of molecular imprinting. The covalent approach.....	16
Figure 2.6. Concept of molecular imprinting. The non-covalent approach. ....	18
Figure 4.1. Synthesis of MAT comonomer. ....	27
Figure 4.2. NMR spectrum of MAT monomer.....	28
Figure 4.3. (A) MAT monomer (B) poly(HEMA-MAT) (C) Chemical structure and 3D-conformation of bilirubin. ....	29
Figure 4.4. FTIR spectra of bilirubin, MAT monomer and MAT-bilirubin complex. ...	30
Figure 4.5. FTIR spectra of NIP and MIP particles.....	30
Figure 4.6. Optic Photographs of the synthesized NIP (left) and MIP(right) particles. ....	31
Figure 4.7. SEM micrographs of MIP (A) and NIP (B) poly(HEMA- MAT) particles.	33
Figure 4.9. Effect of initial bilirubin concentration on adsorption of bilirubin molecules on MIP particles. $V_{total}$ : 10 mL ; 125 mg polymer, time: 60 min, T: 25°C. ....	36
Figure 4.10. Langmuir adsorption isotherm of the MIP particles; T: 25°C. ....	39
Figure 4.11. Freundlich adsorption isotherm of the MIP particles ; T: 25°C. ....	40
Figure 4.12. Pseudo-first-order kinetic of the experimental data for the adsorbent. ...	42
Figure 4.13. Pseudo-second-order kinetic of the experimental data for the adsorbent. ....	42
Figure 4.14. Chemical structures of competitive molecules. ....	44
Figure 4.15. Adsorbed template and competitive molecules both in MIP and NIP particles. 0.8 mg/mL, 10 mL solution, 125 mg polymer, T:25 °C. ....	45
Figure 4.16. Adsorption-desorption cycle of MIP particles. $V_{total}$ : 10 mL ; 125 mg polymer, time: 30 min, T: 25°C.....	46

**TABLE LEGEND**

Table 2.1. Advantages and disadvantages of covalent and non-covalent imprinting. .....	19
Table 4.1. Comparison of the adsorption capacities for bilirubin of various adsorbents .....	37
Table 4.2. Langmuir and Freundlich adsorption isotherm constants .....	41
Table 4.3. The first and second order kinetic constants for the MIP particles. ....	43
Table 4.4. $K_D$ , $k$ , and $k'$ values of cholesterol and testosterone with respect to bilirubin.....	44

## 1. INTRODUCTION

Bilirubin is a tetrapyrrole dicarboxylic acid formed in the normal metabolism of heme proteins in senescent red blood cells, and is normally conjugated with albumin to form a water-soluble complex. It is transported to the liver as a complex with albumin where it is normally conjugated and excreted into the bile [1]. The free bilirubin is toxic. High concentrations of free bilirubin can evoke hepatic or biliary tract dysfunction and permanent brain damage or death in more severe case [2]. Neurological dysfunctions as kernicterus or bilirubin encephalopathy may develop if the bilirubin concentration in the plasma rises above 15 mg/dL. Disorders in the metabolism of bilirubin may cause a yellow discoloration of the skin and other tissues.

Several methods have been developed for the treatment of hyperbilirubinemia such as plasma exchange, hemodialysis, phototherapy and hemoperfusion. Treatment with plasma exchange, however, requires large volumes of fresh frozen plasma, which is expensive and difficult to obtain. Hemoperfusion, i.e., circulation of blood through and extracorporeal column containing and adsorbent system for bilirubin, has become the most promising technique [3-14]. Sideman et al. suggested the application of hemoperfusion to the removal of the bilirubin from jaundiced newborn babies by using albumin deposited macroreticular resin [5]. Idezuki et al. used anion exchange synthetic fibers, and clinically applied this sorbent system in a selective bilirubin separation [6]. Brown prepared oligo-peptide functionalized polyacrylamide particles as affinity sorbent system for bilirubin removal [7]. Chandy et al. used polylysine immobilised chitosan particles for selective bilirubin removal [8]. Yamazaki et al. developed poly(styrene-divinyl benzene) based adsorbents, and successfully applied in the treatment of more than 200 patients with hyperbilirubinemia [9]. Morimoto et al. used plasma exchange and plasma adsorption with styrene-divinyl benzene resin and removed bilirubin from hepatectomized patients [10]. This plasma adsorption system provided a possibility for an improved supportive therapy for hepatic failure, especially for patients with hepatic coma and hyperbilirubinemia. Avramescu et al. conjugated bovine serum albumin with ethylene vinyl alcohol adsorptive membranes and they reported high bilirubin binding capacity [11]. Yu et al. synthesized amine-containing crosslinked chitosan resins and investigated

adsorption behavior of conjugated bilirubin [12]. Kuroda et al studied selective adsorption of bilirubin by macroporous poly(glycidyl methacrylate-co-divinyl-benzene) particles [13]. Ahmad et al. demonstrated the suitability of rat serum albumin loaded poly(lactide-co-glycolide) biodegradable microspheres in removal of bilirubin from systemic circulation of hyperbilirubinemic rats [14]. Denizli et al. showed in in-vitro experiments that dye-affinity adsorbents removed bilirubin from human plasma [15-19].

Highly specific adsorbents underline various affinity-based detection and separation techniques [20]. For example antibodies are routinely utilized as analytical reagents in clinical and research laboratories. For many practical reasons attempts have been made to replace antibodies with more stable counterparts. One technique that is being increasingly adopted for the generation of artificial antibodies is molecular imprinting of synthetic polymers [21]. Given the advantage of easy preparation and chemical stability, molecularly imprinted polymers (MIPs) possess a high potential for use in a variety of applications such as chromatographic stationary phases [22], immunoassay-type analyses [23], metal ion removal studies [24,25] and sensor development [26]. Generally molecular imprinting is a synthetic strategy that is used to assemble a molecular receptor via template-guided synthesis. To prepare MIP, a print molecule (template) is used to guide the assembly of functional monomers. Polymerization reaction is then employed to fix the preassembled binding groups around the print molecule. Following removal of the print molecule, the polymer revealed retains specific binding sites that can selectively rebind the original print molecule. Depending on the interactions between the print molecule and the functional monomers/groups involved at the imprinting and rebinding step, molecular imprinting has two different approaches: non-covalent [27] and covalent [28]. In the non-covalent approach, various non-covalent interactions such as hydrogen bond, ionic interactions and hydrophobic effects are utilized. Given the fact that non-covalent molecular interactions are prevalent in the biological world, exploitation of these binding forces, as it has turned out, has proven to be the most efficient and preferred method for generating robust, biomimetic binding materials [29].

In this work, we have produced MIP particles for the selective removal of bilirubin from hyperbilirubinemic human plasma. Different kinds of MIP particles are manufactured for bilirubin recognition [30-33]. But there are no studies that use MIP

particles for selective bilirubin removal from human plasma. In order to show bilirubin specificity of the MIP particles, competitive adsorptions has also been studied with different molecules (cholesterol and testosterone). Finally, repeated use of the MIP particles for removal of bilirubin molecules from human plasma has been studied as well.

## 2. GENERAL INFORMATION

### 2.1. Bilirubin

A red blood cell has a lifetime of approximately 120 days in adults and 70 days in infants. The active component in a red blood cell is hemoglobin. Hemoglobin is a porphyrin ring with an iron atom in the center. It is able to bind and transport dioxygen to tissues and carbon dioxide to the lungs. When the red blood cell is degraded, iron is recovered but the heme porphyrin ring is degraded into the yellow-orange pigment of bilirubin. The conversion of heme to bilirubin involves two steps. The first step uses heme oxygenase, a monooxygenase, in the presence of dioxygen and NADPH to cleave the alpha methylene. A carbon from a methene bridge is released as carbon monoxide (CO) and the ring structure is opened to produce biliverdin. Biliverdin is the final step in the breakdown of heme for many species of birds, amphibians, and reptiles and is excreted directly. In humans, the central methene bridge of biliverdin is reduced by biliverdin reductase and NADPH to form bilirubin (please see Figure 2.1) .

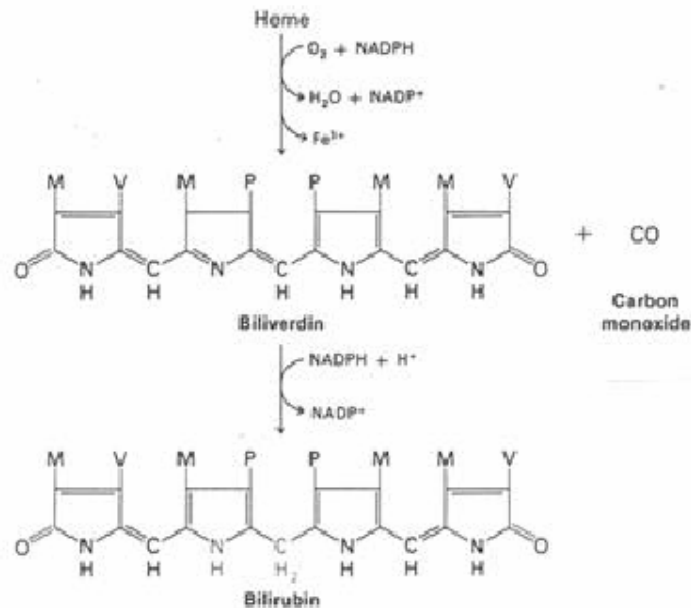


Figure 2.1. Degradation of heme to bilirubin.

Normal plasma bilirubin concentrations are in the range of 5 to 17  $\mu\text{M}$ , where the majority is unconjugated and bound to albumin. The bilirubin-albumin complex is transported to the liver where glucuronate is covalently attached to the propionate

side chains (Stryer, 1986). Glucuronate is similar to glucose but has a  $\text{COO}^-$  at the C-6 position rather than  $\text{CH}_2\text{OH}$ . The conjugate of bilirubin and two glucuronates, called bilirubin diglucuronide, is secreted into the bile (please see Figure 2.2).

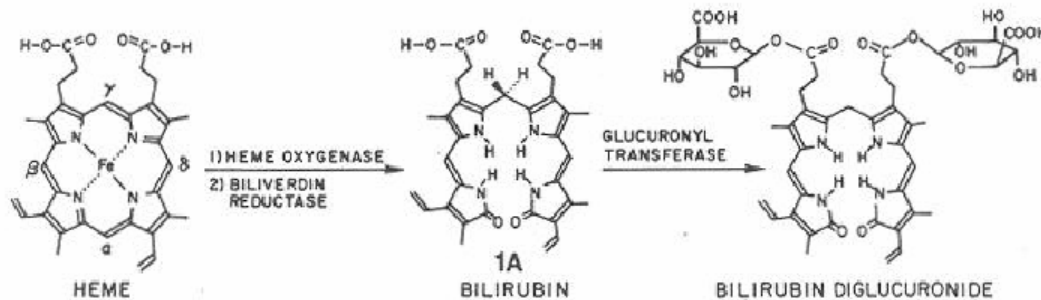


Figure 2.2. Main steps in bilirubin formation and metabolism. (Monoglucuronides are also formed in addition to the diglucuronide structure shown.)

When the bilirubin- glucuronidating enzyme (glucuronyl transferase) is low, only a single bile species, bilirubin, appears in the blood. If the enzyme activity remains depressed then bilirubin will accumulate. Due to its lipophilicity, membrane permeability and its lack of solubility in plasma, bilirubin can be deposited in the tissues, resulting ultimately in clinical jaundice.

Bilirubin can be oxidized by two hydroperoxyl radicals to form biliverdin. Biliverdin can then be reduced back to form bilirubin. On a molar basis, a bilirubin bound albumin is approximately one tenth as effective as ascorbate in affording protection against water-soluble peroxides. In membranes, bilirubin is a highly potent antioxidant similar to vitamin E.

### 2.1.1. Production of Jaundice

Jaundice can occur in neonates and adults, usually under different conditions. Neonatal jaundice is principally transient in nature and can be the result of a deficiency in bilirubin conjugation, hepatic uptake or increased enterohepatic circulation. In adults, jaundice can be a symptom of a larger disease state, for example Crigler-Najjar and cholestasis.

### 2.1.2. Removal of Bilirubin

Bilirubin is only slightly soluble in water at physiological pH and ionic strength. To be transported in the blood, bilirubin must be tightly bound to albumin. When the limited capacity of albumin to bind bilirubin is exceeded; bilirubin is increasingly sequestered in intracellular sites. If plasma concentrations rise above 300  $\mu\text{M}$ , neurological dysfunction called kernicterus or bilirubin encephalopathy may develop. CNS toxicity of bilirubin occurs in two phases: an acute phase reversible by pigment removal and a later phase where problems become irreversible. Neonatal bilirubin removal methods include; exchange transfusion, antibody suppression of hemolysis and inhibition of bilirubin production. Another method of reducing the level of bilirubin is to inhibit production by blocking heme oxygenase by metalloporphyrins.

Bilirubin can be removed by photo-oxidation. Photo-oxidation, involving singlet oxygen and blue light, is able to transform bilirubin into the water-soluble 4Z,15E bilirubin (lumirubin) that is easily excreted (please see Figure 2.3).

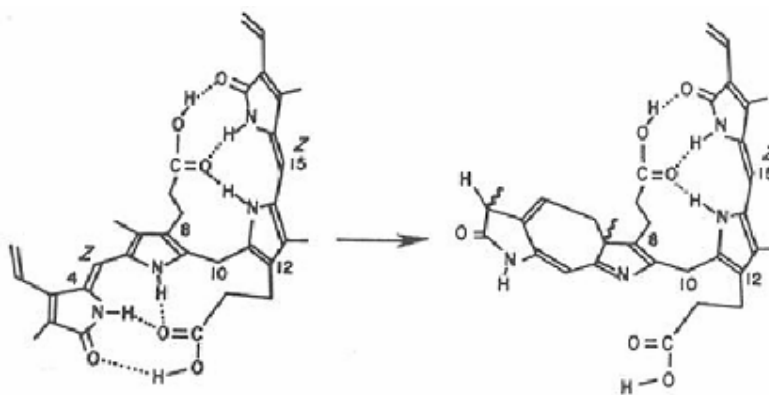


Figure 2.3. Intramolecular cyclization of bilirubin in presence of light to form lumirubin.

### 2.1.3. Detection of Bilirubin

The conventional *in vitro* assay procedure for determining serum bilirubin concentration uses Ehrlich's diazotized sulfanilic acid. This method measures diazo derivatives formed by the reaction of serum bilirubin and diazotized sulfanilic acid. In principle it can determine "direct" reacting (beta and gamma fractions, conjugated

with glucuronate) and “indirect” reacting (alpha, unconjugated) bilirubins. In this assay the delta fraction should not react, as it is covalently bound to albumin. However, this procedure is not very sensitive, as the alpha and delta fractions can be read in the direct reaction. This direct reading can lead to falsely elevated measurements of the conjugated bilirubin levels. A more sensitive method for determining conjugated bilirubin levels is high performance liquid chromatography (HPLC). To determine the sensitivity of this method, rats and guinea pigs were tested under normal conditions and after a bile duct ligation. A bile duct ligation increases the level of conjugated bilirubin in the circulation. Under normal conditions, serum conjugated bilirubin was undetectable (0.006 mg/dl) in rats and guinea pigs. After the bile duct ligation, the HPLC detected elevated rat conjugated bilirubin levels by 10 minutes, whereas the conventional bilirubin measurement did not become significantly elevated until 120 minutes. For the guinea pig, time before detecting elevated results was 30 and 240 minutes, respectively. Micellar electrokinetic chromatography (MEKC) can separate electrically neutral serum bilirubin fractions (alpha, beta, gamma and delta). It can also be used to determine bilirubin oxidase activity and monitor the catalytic reaction.

#### **2.1.4. Bilirubin as an Antioxidant**

An antioxidant interacts with an oxidizing species, itself becoming reduced and changing the oxidant to a less active molecule. Bilirubin can protect albumin from peroxy radical oxidation. A single bilirubin can react with two peroxy radicals, becoming biliverdin. Biliverdin can then become reduced to form bilirubin. Ames et al. have shown that bilirubin bound to albumin can react with peroxy radicals as well as uric acid but not as effectively as vitamin C. They determined that peroxy radicals interacted with bilirubin-albumin 3.1 times faster than uric acid and 12.5 times slower than ascorbate. The antioxidant activity of bilirubin is affected by the concentration of dioxygen. When oxygen was at approximately 20%, bilirubin was able to reduce the rate of oxidation of linoleic acid by about 16%, compared to 10% by  $\beta$ -carotene. However,  $\alpha$ -tocopherol was able to inhibit the initial rate by 97%. With the same concentrations of antioxidants in 2% oxygen (comparable to what is found in tissues) activity of bilirubin increased to 35%. Inhibition by  $\beta$ -carotene was also increased but  $\alpha$ -tocopherol did not change. When these compounds were tested using an aqueous

dispersion of multilamellar liposomes of phosphatidylcholine (a more biologically relevant system)  $\beta$ -carotene, bilirubin and  $\alpha$ -tocopherol inhibited initial rates by 22, 87 and 99%. This data indicates that bilirubin at micromolar concentrations in vitro efficiently scavenges peroxy radicals generated chemically in either homogeneous solution or multilamellar liposomes.

### **2.1.5. Bilirubin and Protein Phosphorylation**

When phosphorylation is inhibited within the cell there can be toxic effects. Phosphorylation of sugars keeps them within the cell. If these sugars are allowed to freely move out of the membrane then energy reserves and starting material for nucleotide synthesis is lost. Bilirubin may inhibit phosphorylation by binding lysine residues. When bilirubin was tested on isolated liver mitochondria in concentrations of  $3 \times 10^{-4}$  M, there was almost a complete inhibition of protein phosphorylation and a partial inhibition of respiration. The concentration of 300  $\mu$ M is also the critical in vivo level where neurological damage in infants is probable. Hansen et al. tested the ability of a polylysine peptide to restore phosphorylation in the presence of bilirubin. They followed the phosphorylation activity of PKA (cAMP-dependent protein kinase). PKA was able to phosphorylate a substrate normally in the presence of 50  $\mu$ M bilirubin when 100  $\mu$ M of polylysine was added [34].

## **2.2. Hemoperfusion**

Hemoperfusion is a treatment technique in which large volumes of the patient's blood are passed over an adsorbent substance in order to remove toxic substances from the blood. Adsorption is a process in which molecules or particles of one substance are attracted to the surface of a solid material and held there. These solid materials are called sorbents. Hemoperfusion is sometimes described as an extracorporeal form of treatment because the blood is pumped through a device outside the patient's body.

The sorbents most commonly used in hemoperfusion are resins and various forms of activated carbon or charcoal.

Hemoperfusion has three major uses:

- to remove nephrotoxic drugs or poisons from the blood in emergency situations (A nephrotoxic substance is one that is harmful to the kidneys.)
- to remove waste products from the blood in patients with kidney disease
- to provide supportive treatment before and after transplantation for patients in liver failure

Hemoperfusion is more effective than other methods of treatment for removing certain specific poisons from the blood, particularly those that bind to proteins in the body or are difficult to dissolve in water. It is used to treat overdoses of barbiturates meprobamate, glutethimide, theophylline, digitalis, carbamazepine, methotrexate, ethchlorvynol, and acetaminophen as well as treating paraquat poisoning. Paraquat is a highly toxic weed killer that is sometimes used by people in developing countries to commit suicide.

A hemoperfusion system can be used with or without a hemodialysis machine. After the patient has been made comfortable, two catheters are placed in the arm, one in an artery and one in a nearby vein. After the catheters have been checked for accurate placement, the catheter in the artery is connected to tubing leading into the hemoperfusion system, and the catheter in the vein is connected to tubing leading from the system through a pressure monitor. The patient is given heparin at the beginning of the procedure and at 15–20-minute intervals throughout the hemoperfusion in order to prevent the blood from clotting. The patient's blood pressure is also taken regularly. A typical hemoperfusion treatment takes about three hours.

Hemoperfusion works by pumping the blood drawn through the arterial catheter into a column or cartridge containing the sorbent material. As the blood passes over the carbon or resin particles in the column, the toxic molecules or particles are drawn to the surfaces of the sorbent particles and trapped within the column. The blood flows out the other end of the column and is returned to the patient through the tubing attached to the venous catheter. Hemoperfusion is able to clear toxins from a larger

volume of blood than hemodialysis or other filtration methods; it can process over 300 mL of blood per minute.

Many techniques have been used for the bilirubin removal from plasma of patients suffering from hyperbilirubinemia. Phototherapy is one of the most commonly used treatments for mild cases. However, severe cases must be treated by more drastic methods, such as hemodialysis and hemoperfusion. Now, hemoperfusion, i.e., circulation of blood through an extracorporeal unit containing an adsorbent system for bilirubin, has become the most promising technique. Successful hemoperfusion requires the adsorbents to be specific; have high adsorption capacity and good blood compatibility; not be poisonous. Highly specific adsorbents underline various affinity-based detection and separation techniques. For example biological antibodies are routinely utilized as analytical reagents in clinical and research laboratories. For many practical reasons attempts have been made to replace antibodies with more stable counterparts. One technique that is being increasingly adopted for the generation of artificial antibodies is molecular imprinting of synthetic polymers . [35].

## **2.3. Molecular Imprinting**

### **2.3.1. Naturally Occurring Receptors**

There are many cells and molecules in our body, and all of them are cooperatively working in an enormously ordered fashion. Without such mutual understanding and cooperation, we cannot survive. Thus, molecular recognition is essential for the existence of life. For example, the receptors on the surface of cell membranes bind hormones and are responsible for cell-to-cell communication. When the receptor binds a hormone, its conformation is changed and the message of the hormone is passed to the cell in terms of this conformational change. Now that this cell knows what is required in the body at that moment, it promotes (or suppresses) the corresponding bioreaction(s) to respond to this requirement appropriately. In the above example, glycogen is hydrolyzed and glucose is supplied to the body. The most important thing in these systems is that one receptor accepts only one specific hormone and never significantly interacts with others. Furthermore, this receptor/hormone interaction is enormously strong. Thus, even small amount of

hormone can correctly deliver its information to the target cell without information cross talk between cells. On the other hand, selective guest binding by antibodies is essential for our immune response. These proteins patrol around in our body like policemen, arrest a foreign substance (antigen) when it enters the body, and take it to a lysosome (a cell organelle) where the antigen is destroyed. Our body is successfully protected. As would be expected, the differentiation by an antibody between the target antigen and the others (and also between foreign substances and the intrinsic ones in our body) must be rigorously strict.

As is well known, enzymes also show high substrate specificity. Each of them exclusively chooses a certain substrate (specific substrate) and transforms it into a predetermined product. All other compounds in the system (even if they resemble the specific substrate) are kept intact. Another enzyme takes another specific substrate and executes a different mission. This substrate specificity primarily comes from selective guest binding by substrate-binding sites of enzymes. Furthermore, only the specific substrate is efficiently transformed into the desired products, since the catalytically active amino acid residues of enzymes, located near the substrate-binding sites, are arranged suitably only for this transformation.

Detailed information on molecular recognition in nature is now available from X-ray crystallography and NMR spectroscopy. The substrate-binding sites of enzymes are apolar pockets or clefts, which are formed from a number of amino acid residues. There, several functional groups (OH, NH<sub>2</sub>, COOH, imidazole, main-chain amide groups, and others) are precisely placed to interact with the functional groups of a specific substrate. For example, an ammonium ion of an enzyme shows Coulomb interaction with a negatively charged carboxylate of its specific substrate. A hydrogen bond is formed between the OH residues of the enzyme and the substrate. Furthermore, apolar binding occurs between them. For the specific substrate only, all these interactions satisfactorily and cooperatively operate, and a stable non-covalent complex is formed. Antibody-antigen interactions, as well as guest binding by membrane-receptors, occur essentially in the same manner. A number of amino acid residues of antibodies (or receptors) are oriented complementarily to the functional groups of the target antigens (or hormones). Precise molecular recognition also occurs when proteins interact with each other.

### 2.3.2. Artificial Receptors

The elegance of molecular recognition in nature has been spurring many scientists to mimic it. One of the greatest advantages of artificial receptors over naturally occurring ones is freedom of molecular design. Their frameworks are never restricted to proteins, and a variety of skeletons (e.g., carbon chains and fused aromatic rings) can be used. Thus the stability, flexibility, and other properties are freely modulated according to need. Even functional groups that are not found in nature can be employed in these man-made compounds. Furthermore, when necessary, the activity to respond towards outer stimuli (photo-irradiation, pH change, electric field, and others) can be provided by using appropriate functional groups. The spectrum of functions is far wider than that of naturally occurring ones.

Pioneering works by Cram, Lehn, and Pedersen (Nobel Prize winners in 1987) established that the following factors are necessary for accurate molecular recognition.

1. Functional residues of guest and receptor must be complementary to each other.
2. Conformational freedom of both components should be minimized.
3. Chemical circumstances should be appropriately related.

In many cases, various functional residues are covalently attached to cyclic host molecules (e.g., cyclodextrins and crown ethers). Although each of the interactions (hydrogen-bonding, electrostatic and apolar-binding) is rather weak, remarkably high selectivities and binding strengths are accomplished when all of them work cooperatively. Alternatively, functional residues are bound to carbon skeletons so that they converge to the central guest binding portion. In principle, good receptors can be successfully synthesized, as long as (i) we are not concerned about cost and time for their preparation, (ii) our target guest is fairly small, and (iii) we can use organic solvents for the guest recognition. However, these conditions are hardly ever fulfilled, making the molecular imprinting method significant and attractive.

### **2.3.3. Receptors for Practical Applications**

In industry, receptors are being used to separate the target product economically from reaction mixtures and to remove dangerous chemicals from waste-water. Applications to molecular biology (regulation of bioreactions, separation of biomaterials, and others) are also promising. In some cases, the cost of the separation of the product and its purification accounts for more than half of the total cost of production. Thus, highly selective and economical receptors are crucially important for successful business. Furthermore, unprecedentedly compact and sophisticated devices are fabricated by placing molecules in an ordered fashion. Here, precise recognition between molecules is essential. Molecular memories, molecular devices, and molecular machines have been already realized to some extent (Lehn, 1995; Amabilino and Stoddart, 1995; Koumura, et al., 1999; Shigekawa, et al., 2000) It is also said that artificial cells could be prepared in the near future by placing man-made receptors on artificial cell membranes.

When we design new receptors for future applications, the following factors must be carefully considered.

1. Easy preparation in large amounts at low cost.
2. Stability and activity under wide operation conditions.
3. Selective and strong binding toward large guest molecules.
4. Guest binding in water.

The first and the second requirements are trivial The third one comes from the fact that important molecules in advanced sciences (proteins, nucleic acids, polysaccharides, bioactive chemicals, and others) are usually large. The fourth requirement has been rapidly increasing in importance, since economical, ecological, and environmental restraints are spurring the replacement of organic solvents with water. For biotechnology, of course, the solvent must be water.

### **2.3.4. The Importance of the Molecular Imprinting Method**

The molecular imprinting method is quite simple and easy to perform in a tailor-made fashion. All we need are functional monomers, templates, solvents, and cross linking

agents. Polymerization is followed by the removal of the template. During these processes, a number of functional monomers are assembled in an orderly fashion and their functional groups are placed at the desired sites in the cavities of desired size. Neither complicated organic synthesis nor complex molecular design is necessary. If you wish to have a receptor toward a certain guest compound, you can simply polymerize appropriate monomer(s) in the presence of this guest compound (or its analog) as the template. For another guest, you can use another combination of functional monomer and template. The corresponding receptor can be at hand almost automatically. Requirements 1 and 2 would seem to be sufficiently fulfilled. Furthermore, significant progress has recently been made in the fulfillment of requirements 3 and 4. This methodology certainly opens the way to further developments in science and technology.

### **2.3.5. General Principle of Molecular Imprinting**

Suppose that a number of functional molecules interact with a template molecule in solution (or in a gas). The interactions are hydrogen-bonding, electrostatic, apolar, and any other non-covalent interactions. Here, these functional molecules are arranged in an orderly manner with respect to each other so that their functional groups are complementary to the template. Then, what happens if we suddenly remove the template molecule from this system? As you can easily imagine, all the functional molecules would soon start moving randomly, and their ordering would disappear. As a result, the memory about the template is immediately gone. In the molecular imprinting method, however, this randomization is minimized by connecting these functional molecules together by means of a polymer backbone (Figure 2.4). A kind of snapshot of solution (or gas) is taken, and the structure of the template is memorized in these polymers, providing the target receptors.

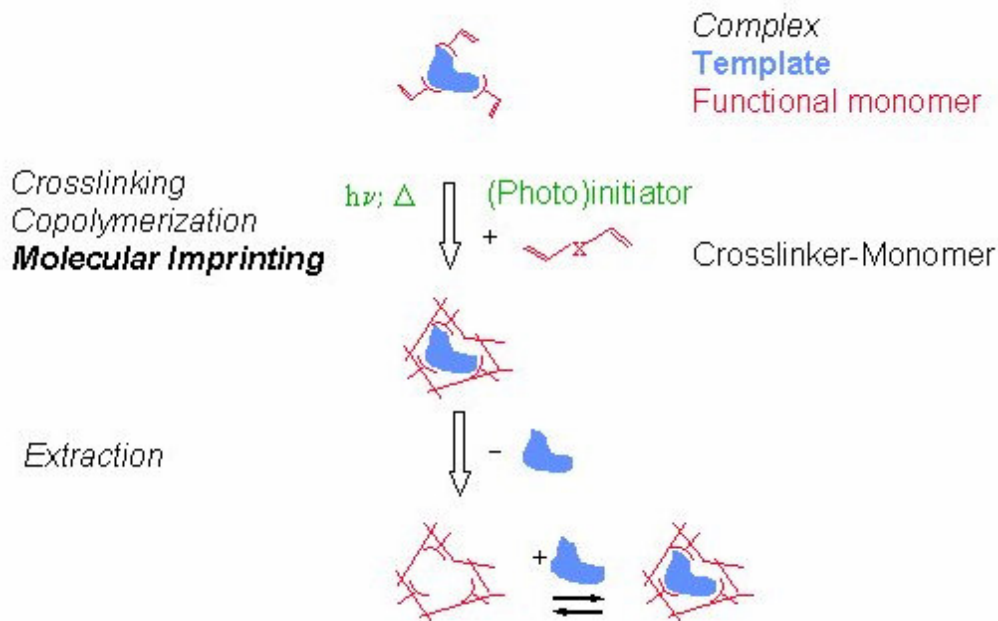


Figure 2.4. Schematic illustration of molecular imprinting

Molecular imprinting processes are composed of the following three steps:

1. Preparation of covalent conjugate or non-covalent adduct between a functional monomer and a template molecule,
2. Polymerization of this monomer-template conjugate (or adduct), and
3. Removal of the template from the polymer.

In step 1, functional monomer and template are connected by a covalent linkage (in covalent imprinting) or they are placed nearby through non-covalent interactions (in non-covalent imprinting). In step 2, the structures of these conjugates (or adducts) are frozen in a three-dimensional network of polymers. The functional residues (derived from the functional monomers) are topographically complementary to the template. In step 3, the template molecules are removed from the polymer. Here, the space in the polymer originally occupied by the template molecule is left as a cavity. Under appropriate conditions these cavities satisfactorily remember the size, structure, and other physicochemical properties of the template, and bind this molecule (or its analog) efficiently and selectively.

### 2.3.6. Covalent Imprinting and Non-covalent Imprinting

As described above, the molecular imprinting method is of two types, depending on the nature of adducts between functional monomer and template (either covalent or non-covalent). Typical examples of these two kinds of methods are presented in Figures 2.5 and 2.6 both have advantages and disadvantages, and thus the choice of the best method strongly depends on various factors (see below).

#### 2.3.6.1. Covalent Imprinting

Wulff and his coworkers reported the first covalent imprinting shown in Figure 2.5 in 1997. They synthesized 2:1 covalent conjugate of p-vinylbenzeneboronic acid with 4-nitrophenyl- $\alpha$ -D-mannopyranoside (the template), and copolymerized this conjugate with methyl methacrylate ethylene dimethacrylate (a crosslinking monomer). After the polymerization, the boronic acid ester in the polymer was cleaved, and the 4-nitrophenyl- $\alpha$ -D-mannopyranoside was removed.

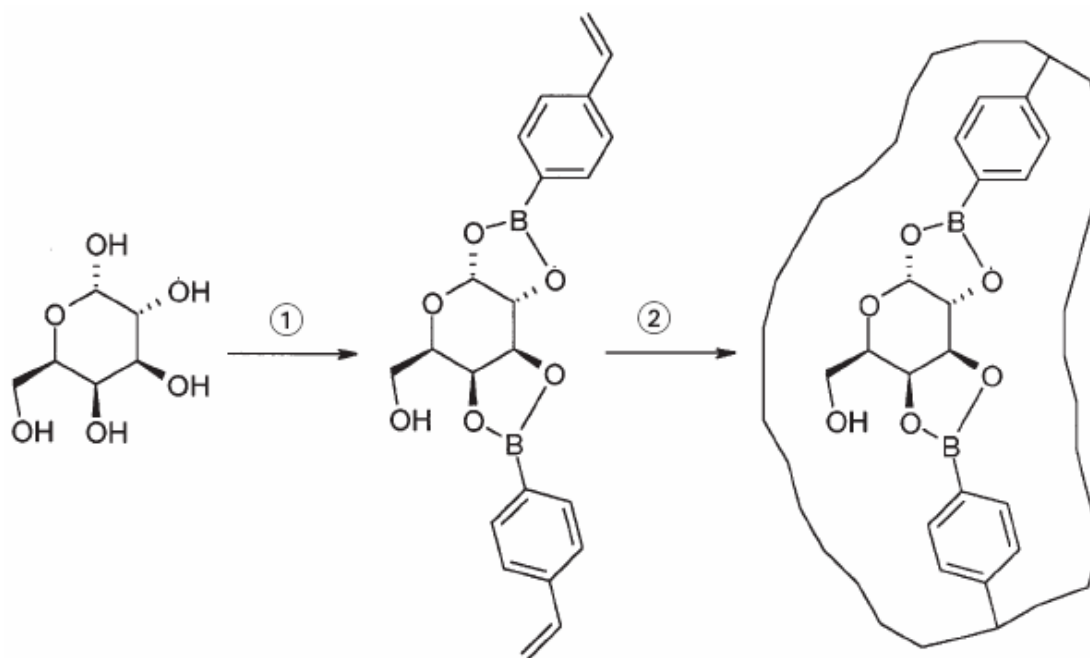


Figure 2.5. Concept of molecular imprinting. The covalent approach.

Exactly as desired, the resultant polymer strongly and selectively bound this sugar. The mutual conformation of the two boronic acid groups in the covalent conjugate

were frozen in the polymer, and the structure of the template was memorized. Similarly, Shea formed a ketal conjugate between carbonyl group of a template and the 1,3-diol group in a functional monomer, and used this covalent conjugate for molecular imprinting.

Prior to polymerization, functional monomer and template are bound to each other by covalent linkage (step 1). Then, this covalent conjugate is polymerized under the conditions where the covalent linkage is intact (step 2). After the polymerization, the covalent linkage is cleaved and the template is removed from the polymer. A typical example of this method is presented in Figure 2.5.

#### **2.3.6.1.1. Advantages of Covalent Imprinting**

1. Monomer-template conjugates are stable and stoichiometric, and thus the molecular imprinting processes (as well as the structure guest-binding sites in the polymer) are relatively clear-cut.
2. A wide variety of polymerization conditions (e.g., high temperature high or low pH, and highly polar solvent) can be employed, since the conjugates are formed by covalent linkages and are sufficiently stable.

#### **2.3.6.1.2. Disadvantages of Covalent Imprinting**

1. Synthesis of the monomer-template conjugate is often troublesome and less economical.
2. The number of reversible covalent linkages available is limited.
3. The imprinting effect is in some case diminished in step 3 (cleavage of covalent linkages), which requires rather severe conditions.
4. Guest binding and guest release are slow, since they involve the motion and breakdown of a covalent linkage.

### 2.3.6.2. Non-covalent Imprinting

Mosbach and his coworkers showed that covalent linkages between functional monomer and template are not necessarily required for molecular imprinting, and even non-covalent interactions between them work sufficiently. Simply by mixing those in a reaction mixture, their non-covalent adducts were spontaneously formed, and satisfactory imprinting effects were obtained. In the imprinting of methacrylic acid with theophylline (a drug), for example, a non-covalent monomer-template adduct was formed through hydrogen bonding and electrostatic interaction (Figure 2.6). The same strategy was successful for the imprinting with various drugs, insecticides, and other practically important chemicals. Many experimental workers were surprised to see that the methods are so simple while the imprinting effects are so remarkable. They were soon persuaded that this method is satisfactorily applicable to a wide range of molecules and started to use it in their own laboratories.

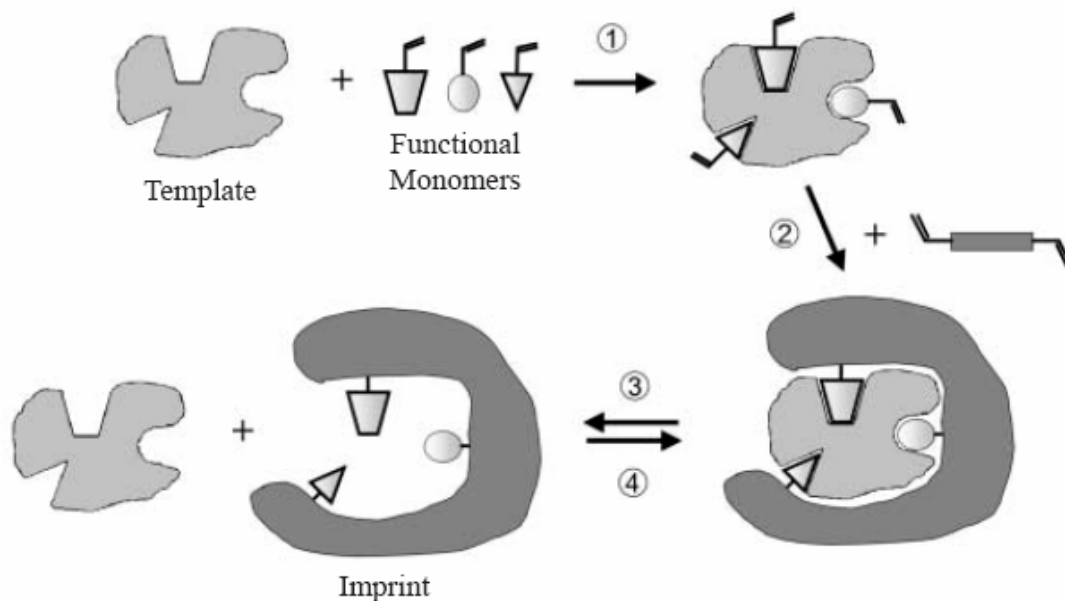


Figure 2.6. Concept of molecular imprinting. The non-covalent approach.

In order to connect a functional monomer with a template, non-covalent interactions (e.g., hydrogen bonding, electrostatic interaction, and coordination-bond formation) are used here. Thus, the adducts can be obtained in-situ simply by adding the components to reaction mixtures (step 1). After the polymerization (step 2), the template is removed by extracting the polymer with appropriate solvents (step 3). The

guest binding by the polymer occurs through the corresponding non-covalent interactions (step 4).

### **2.3.6.2.1. Advantages of Non-covalent imprinting**

1. Synthesis of covalent monomer-template conjugates is unnecessary.
2. Template is easily removed from the polymer under very mild conditions, since it is only weakly bound by non-covalent interactions.
3. Guest binding and guest release, which take advantage of non-covalent interactions, are fast.

### **2.3.6.2.2. Disadvantages of Non-covalent imprinting**

1. The imprinting process is less clear-cut (monomer-template adduct is labile and not strictly stoichiometric).
2. The polymerization conditions must be carefully chosen to maximize the formation of non-covalent adduct in the mixtures.
3. The functional monomers existing in large excess (in order to displace the equilibrium for adduct-formation) often provide nonspecific binding sites, diminishing the binding selectivity.

Table 2.1. Advantages and disadvantages of covalent and non-covalent imprinting.

	Covalent	Non-covalent
Synthesis of monomer-template conjugate	Necessary	Unnecessary
Polymerization condition	Rather free	Restricted
Removal of template after polymerization	Difficult	Easy
Guest-binding and guest-release	Slow	Fast
Structure of guest-binding site	Clearer	Less clear

### **2.3.7. Hybridization of Covalent Imprinting and Non-covalent Imprinting**

The advantage of covalent imprinting (clear-cut nature) and that of non covalent imprinting (fast guest binding) were combined. The polymers were prepared as in covalent imprinting, but the guest binding employed non-covalent interactions (Figure 2.6). One of the shortcomings of covalent imprinting (slow guest binding and guest release) has been solved by this approach. Nowadays, the molecular imprinting method is being widely used to place the target molecules at desired sites easily and economically. The purpose is not restricted to the preparation of artificial receptors and is much wider in scope. There are no alternative methods which can freeze molecular movements in solutions (or in gases) and immobilize them according to design. The use of biomolecules as templates is also promising in molecular biology and pharmacology [36-38].

### 3. EXPERIMENTAL

#### 3.1. MATERIALS

Bilirubin, cholesterol, testosterone, L-tyrosine methylester, methacryloyl chloride, were supplied by Sigma (St Louis, USA). Hydroxyethyl methacrylate and ethylene glycol dimethacrylate (EGDMA) were also obtained from Sigma (St Louis, USA), distilled under reduced pressure in the presence of hydroquinone inhibitor and stored at 4°C until use.  $\alpha$ - $\alpha'$ -azobisisobutyronitrile (AIBN) was obtained from Fluka (Switzerland). Methanol and acetonitrile were HPLC grade and were supplied from Sigma (St Louis, USA). All other chemicals were of reagent grade and were purchased from Merck AG (Darmstadt, Germany). All water used in the experiments was purified using a Barnstead (Dubuque, IA) ROPure LP<sup>®</sup> reverse osmosis unit with a high flow cellulose acetate membrane (Barnstead D2731) followed by a Barnstead D3804 NANOpure<sup>®</sup> organic/colloid removal and ion exchange packed-bed system. Buffer and sample solutions were prefiltered through a 0.2  $\mu$ m membrane (Sartorius, Göttingen, Germany). All glassware was extensively washed with dilute nitric acid before use.

#### 3.2. PREPARATION OF POLYMERIC PARTICLES

##### 3.2.1. Synthesis of N-Methacryloyl-(L)-Tyrosine

The MAT was selected as the functional monomer for bilirubin imprinting. The following experimental procedure was applied for the synthesis of MAT. 5.0 g of L-tyrosine methylester and 0.2 g of hydroquinone were dissolved in 100 mL of dichloromethane solution. This solution was cooled down to 0°C. 12.7 g triethylamine was added to the solution. 5.0 mL of methacryloyl chloride was poured slowly into this solution and then it was stirred magnetically at room temperature for 2 h. At the end of the chemical reaction period, hydroquinone and unreacted methacryloyl chloride were extracted with 10% NaOH solution. Aqueous phase was evaporated in a rotary evaporator. The residue (i.e., MAT) was crystallized in an ether-cyclohexane mixture and then dissolved in ethyl alcohol.

### 3.2.2. Preparation of Bilirubin Imprinted Poly(HEMA-MAT) Particles

In the first part, MAT-bilirubin complex was prepared. Briefly, N-methacryloyl-(L)-tyrosine methylester (MAT) (4 mg) was dissolved in sodium carbonate and sodium hydroxide solution. ( $\text{Na}_2\text{CO}_3$ , 0.1 M, NaOH 0,1 M ), then bilirubin (2 mg) was added in this solution. Then the bilirubin-monomer complex was used in the polymerization procedure. Hydroxyethyl methacrylate (HEMA) and bilirubin-MAT complex were polymerized in bulk polymerization by using ammonium persulphate (APS) as the initiator. Toluene and ethylene glycol dimethacrylate (EGDMA) was included in the polymerization recipe as the pore former and cross-linker, respectively. N,N,N',N'-Tetraethyldiethylene-triamine (TEMED) was used as the activator. Ammonium persulfate (20 mg) and TEMED (100  $\mu\text{L}$ ) were dissolved in the mixture of monomers (HEMA: 1.0 mL, bilirubin-MAT complex: 500  $\mu\text{l}$ , EGDMA: 500  $\mu\text{l}$ ) and porogenic diluent (toluene: 500  $\mu\text{l}$ ). The polymerization mixture was poured in a glass tube and sealed after purging with nitrogen for 2 min. Polymerization reaction was completed in 10 minutes at room temperature. At the end of the polymerization reaction, soluble components were removed from the polymer by repeated decantation with water and methanol. Bilirubin imprinted poly(HEMA-MAT) (MIP) bulk polymer was ground in a mill after drying and washed several times with methanol and water to remove any unreacted components completely. Washed particles were ground again and sieved through 100  $\mu\text{m}$  sieves (Retsch Standard Sieves -Model AS200, Retsch GmbH & Co, KG, Haan, Germany). Non-imprinted particles (NIP, i.e poly(HEMA-MAT) particles) were prepared in the same manner as above only without using bilirubin as template. Note that all bilirubin adsorption studies were done at dark place in order to minimize the transformation of bilirubin to biliverdin.

### 3.2.3. Removal of the Template (Bilirubin)

In order to remove unreacted monomers and other ingredients, MIP particles were extensively washed with methanol/water solution (60/40, v/v) for 24 h at room temperature in dark room. After cleaning procedure, the template was removed from the polymer particles using 2 M NaOH and 2 M  $\text{Na}_2\text{CO}_3$  includes EDTA solution. Molar ratio of NaOH and EDTA was 4:1. The imprinted particles were added into the solution system for 48 h at room temperature in dark room. This procedure was

repeated until no bilirubin leakage was observed from the MIP particles to the wash solution. The template free particles were cleaned with ethanol and water in a magnetic stirrer at room temperature for 12 h.

### **3.3. CHARACTERIZATION OF PARTICLES**

#### **3.3.1. Swelling Test**

Swelling ratios of NIP and MIP particles were determined in distilled water and toluen: chloroform mixture (7:1 v/v). The experiment was conducted as follows: initially dry particles were carefully weighed ( $\pm 0.0001$  g) before being placed in a 50 mL vial containing swelling medium. The vial was put into an isothermal water bath with a fixed temperature ( $25 \pm 0.5^\circ\text{C}$ ) for 2 h. The polymer sample was taken out from the medium, wiped using a filter paper, and weighed. The weight ratio of dry and wet samples was recorded. The swelling ratio was calculated by using the following expression:

$$\text{Swelling ratio \%} = [(W_S - W_0) / W_0] \times 100 \quad (3.1)$$

Where,  $W_0$  and  $W_S$  are the weights of particles before and after swelling, respectively.

#### **3.3.2. Surface Morphology**

The surface morphology of the particles was examined using scanning electron microscopy (SEM). The samples were initially dried in air at  $25^\circ\text{C}$  for seven days before being analyzed. A fragment of the dried particles was mounted on a SEM sample mount and was sputter coated for 2 minutes. The sample was then mounted in a SEM (JEOL, JEM 1200EX, Tokyo, Japan). The surface of the sample was then scanned at the desired magnification to study the particles.

#### **3.3.3. Elemental Analysis**

To evaluate the degree of MAT incorporation to the polymer structure, particles were subjected to elemental analysis using a Leco Elemental Analyzer (Model CHNS-932, USA).

### 3.3.4. FTIR Studies

FTIR spectra of MAT, bilirubin and MIP particles were obtained by using a FTIR spectrophotometer (FTIR 8000 Series, Shimadzu, Japan). The dry sample (about 0.1 g) was thoroughly mixed with KBr (0.1 g, IR Grade, Merck, Germany), and pressed into a pellet form and the FTIR spectrum was then recorded.

### 3.3.5. NMR Studies

$^1\text{H}$  NMR spectroscopy was used to determine the structure of MAT. The  $^1\text{H}$  NMR spectrum of MAT monomer was taken in DMSO- $\text{D}_6$  on a Bruker-400 MHz instrument (USA). The residual non-deuterated solvent (DMSO) served as an internal reference. Chemical shifts are reported in ppm ( $\delta$ ) downfield relative to solvent.

## 3.4. ADSORPTION-DESORPTION STUDIES

### 3.4.1. Bilirubin Removal From Human Plasma

Bilirubin removal from human plasma was studied in a batch system. Blood samples taken from a patient with hyperbilirubinemia was used in bilirubin adsorption studies. Human blood was collected from thoroughly controlled voluntary blood donors. Each unit should be separately controlled and found negative for HBS antigen, HIV type I and II and hepatitis C antibodies. No preservatives were added to the blood samples. Human blood samples were transferred into EDTA-containing vacutainers in which red blood cells were separated from plasma by centrifugation at 4000 g for 30 min at room temperature, then filtered off through a 0.45  $\mu\text{m}$  syringe filters (Model 245-0045 Nalgen Co., Rochester, New York) and the plasma was deep-frozen at  $-20^\circ\text{C}$ . Before use, the plasma was thawed slowly for over 1 h at  $37^\circ\text{C}$ . All adsorption experiments were carried out in a dark room. In a typical adsorption system, 10 mL of the human plasma was incubated with a 125 mg of particles, at  $20^\circ\text{C}$  for 2 h. The concentration of the bilirubin molecules in the plasma after the desired treatment periods was measured by using Roche Hitachi Modular-P with using Roche Bilirubin Direct, Indirect Test Kits. The experiments were performed in replicates of three and the samples were analyzed in replicates of three as well. For each set of data

present, standard statistical methods were used to determine the mean values and standard deviations. Confidence intervals of 95% were calculated for each set of samples in order to determine the margin of error. The amount of bilirubin adsorption per unit mass of the particles was evaluated by using the following expression:

$$Q = [(C_0 - C) \cdot V] / m \quad (3.2)$$

Here,  $q$  is the amount of bilirubin adsorbed onto unit mass of the particles (mg/g);  $C_0$  and  $C$  are the concentrations of the bilirubin in the initial plasma and in the plasma after treatment for certain period of time, respectively (mg/mL);  $V$  is the volume of the solution (L); and  $m$  is the mass of the particles used (g).

### 3.4.2. Selectivity Experiments

In order to show bilirubin molecules specificity of MIP particles, competitive adsorption (i.e., cholesterol; MW: 386 g/mol, testosterone; MW: 288 g/mol) was also studied. 10 mL of fresh human plasma was overloaded with cholesterol and testosterone by the same procedure. MIP particles were treated with the competitive molecules. After adsorption equilibrium, the concentrations of cholesterol and testosterone in the remaining solution were measured by Roche Hitachi Modular-P, with Roche Direct Bilirubin, Indirect Bilirubin Test Kit.

Distribution and selectivity coefficients of cholesterol and testosterone with respect to bilirubin were calculated as explained by the following Eq. 3.3.

$$K_d = [(C_i - C_f) / C_f] \times V / m \quad (3.3)$$

Here,  $K_d$  represents the distribution coefficient;  $C_i$  and  $C_f$  are the initial and final concentrations of biomolecules, respectively.  $V$  is the volume of the solution (mL) and  $m$  is the mass of particles used (g).

The selectivity coefficient for the binding of bilirubin in the presence of other biomolecules (Eq. 3.4) can be obtained from equilibrium binding data according to (Eq. 3.5).



$$K = ([M_2]_{\text{solution}} [M_1]_{\text{sorbent}}) / ([M_1]_{\text{solution}} [M_2]_{\text{sorbent}}) \quad (3.5)$$

$$= K_d (\text{bilirubin}) / (K_d (X))$$

Where  $k$  is the selectivity coefficient and  $X$  represents cholesterol and testosterone molecules. A comparison of the  $k$  values of the MIP particles with those steroid molecules allows an estimation of the effect of imprinting on selectivity.

A relative selectivity coefficient  $k'$  (Eq. 3.6) can be defined as

$$k' = k_{\text{imprinted}} / k_{\text{control}} \quad (3.6)$$

### 3.2 DESORPTION AND REPEATED USE

Desorption of bilirubin molecules were studied with two different desorption agent; 2 M NaOH (contained EDTA with the molar ratio NaOH:EDTA 4:1), and 2 N Na<sub>2</sub>CO<sub>3</sub> solution, respectively. MIP particles were placed in this desorption medium and stirred continuously (at a stirring rate of 400 rpm) for 2 h at room temperature. The final bilirubin concentration in the desorption medium was measured by Roche Hitachi Modölar-P with using Roche Bilirubin Direct, Indirect Test Kits. The desorption ratio was calculated from the amount of bilirubin adsorbed on the particles and the final bilirubin concentration in the desorption medium by the following Equation (Eq. 3.7).

$$\text{Desorption Ratio} = \frac{\text{amount of bilirubin desorbed to the elution medium}}{\text{amount of bilirubin adsorbed on the particles}} \times 100 \quad (3.7)$$

In order to test the reusability of the MIP particles, bilirubin adsorption-desorption procedure was repeated five times by using the same MIP adsorbent. In order to regenerate and sterilize, after desorption; the particles were washed with 50 Mm NaOH solution.

## 4. RESULTS AND DISCUSSION

### 4.1. Characterization of Bilirubin-Imprinted Particles

The functional comonomer, (N)-methacryloyl-(L)-tyrosine (MAT) was synthesized from the reaction of (L)-tyrosine and methacryloyl chloride (Figure 4.1).

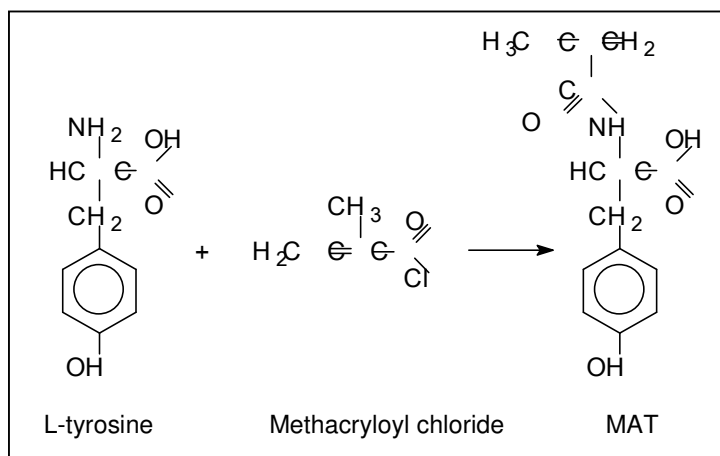


Figure 4.1. Synthesis of MAT comonomer.

The obtained MAT comonomer <sup>1</sup>H-NMR spectrum was shown in Figure 4.2. The characteristic peaks from the groups in MAT monomer of related protons are marked on the spectrum. These characteristic peaks are as follows: 2.05 ppm 3H singlet (-C=C-CH<sub>3</sub>, vinyl methyl **(a)**), 5.4-5.7 ppm 2H (-C=CH<sub>2</sub>) **(b)**, 3.65 ppm 2H (-CH<sub>2</sub>-C-) **(c)**, 4.5 ppm 1H (-CH-C-) **(d)**, 8.2 ppm 1H (amine protons) **(f)**, 6.6-7.1 ppm aromatic protons **(g)**. Carboxyl proton was observed between 9.0-10.0 ppm as a large peak **(e)**. DMSO-D<sub>6</sub> was used as solvent.

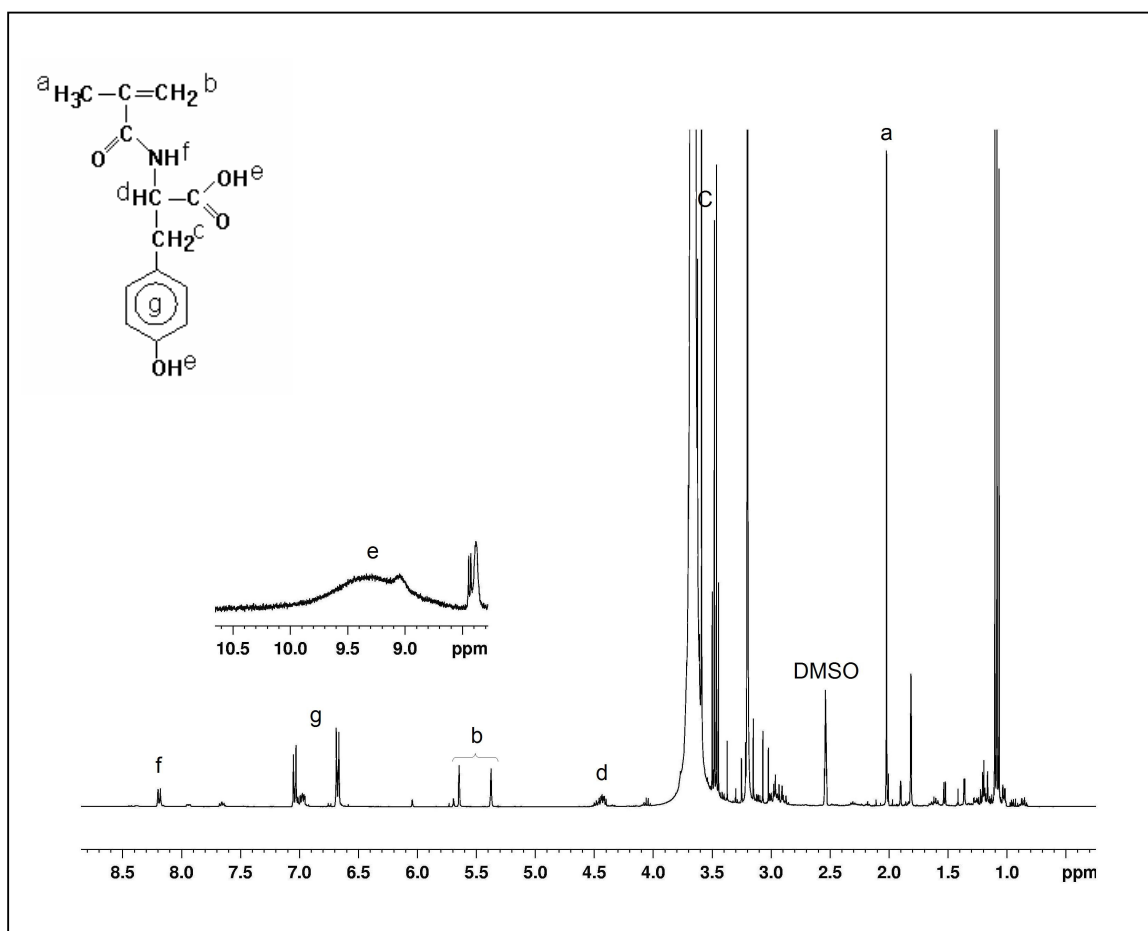


Figure 4.2. NMR spectrum of MAT monomer.

MAT was selected as the functional comonomer for the selective separation of bilirubin. The molecular formula of synthesized MAT comonomer, bilirubin and copolymer is shown in Figure 4.3. FTIR spectra of MAT monomer, bilirubin molecule, MAT-bilirubin complex monomer, bilirubin imprinted (MIP) and non-imprinted (NIP) poly(HEMA-MAT) particles are shown in Figure 4.4 and Figure 4.5, respectively. FTIR spectrum of pure bilirubin has two important characteristic peaks include N-H amine at  $3406\text{ cm}^{-1}$  and pyrrole at  $755\text{ cm}^{-1}$ . FTIR spectrum of MAT has the characteristic stretching vibration amide I and amide II absorption bands at  $1653\text{ cm}^{-1}$  and  $1516\text{ cm}^{-1}$ , and carbonyl band at  $1733\text{ cm}^{-1}$  and aromatic C-H at  $809\text{ cm}^{-1}$  as shown in Figure 4.4. Functional monomer MAT is expected to interact with bilirubin through H-bonds and hydrophobic interactions through aromatic ring. In MAT-bilirubin monomer complex, pyrrole at  $755\text{ cm}^{-1}$ , which is the characteristic peak of bilirubin is seen apparently. Furthermore, the aromatic peak at  $809\text{ cm}^{-1}$  of MAT monomer shifts

upper field to  $813\text{ cm}^{-1}$  due to hydrophobic interactions. MIP and NIP particles give similar peaks as shown in Figure 4.5. They were synthesized at same conditions and they have similar functional groups. The characteristic peak bilirubin, pyrrole at  $755\text{ cm}^{-1}$  which is the only evidence of imprinting of bilirubin appeared too noisy and could not be identified in fingerprint region of MIP particles. It should be noted that peak intensities were decreased in the resulting polymer. By the way, Figure 4.6. represents the optic photographs of NIP (left) and MIP(right) particles. It is clearly seen that the MIP particles have a characteristic yellow-green bilirubin color.

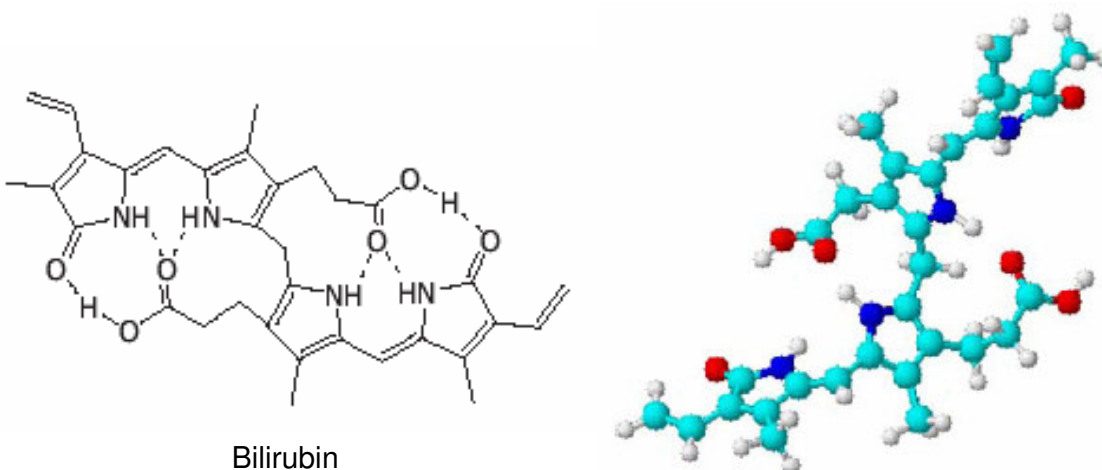
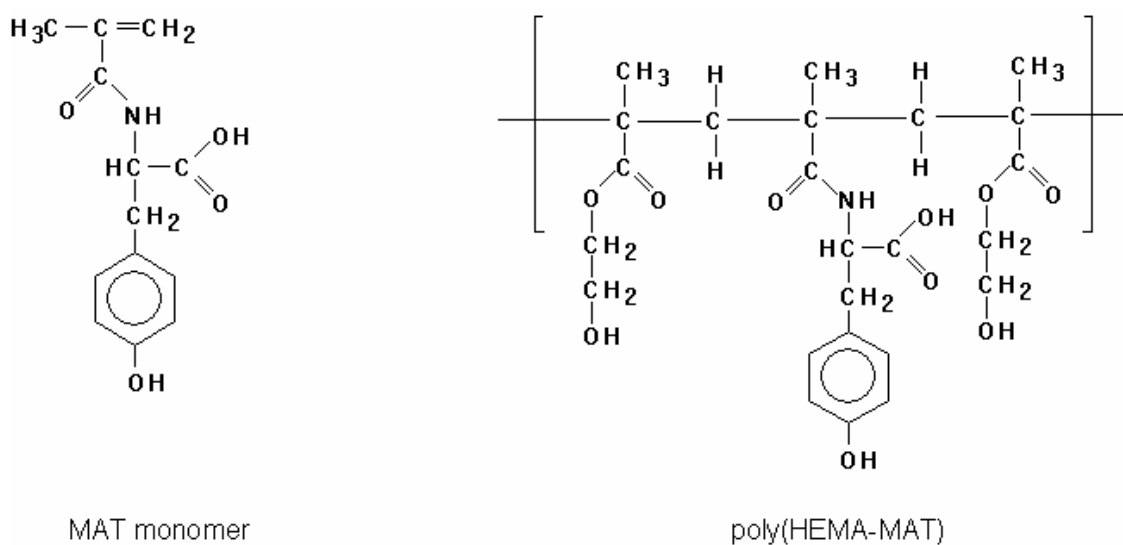


Figure 4.3. (A) MAT monomer (B) poly(HEMA-MAT) (C) Chemical structure and 3D-conformation of bilirubin.

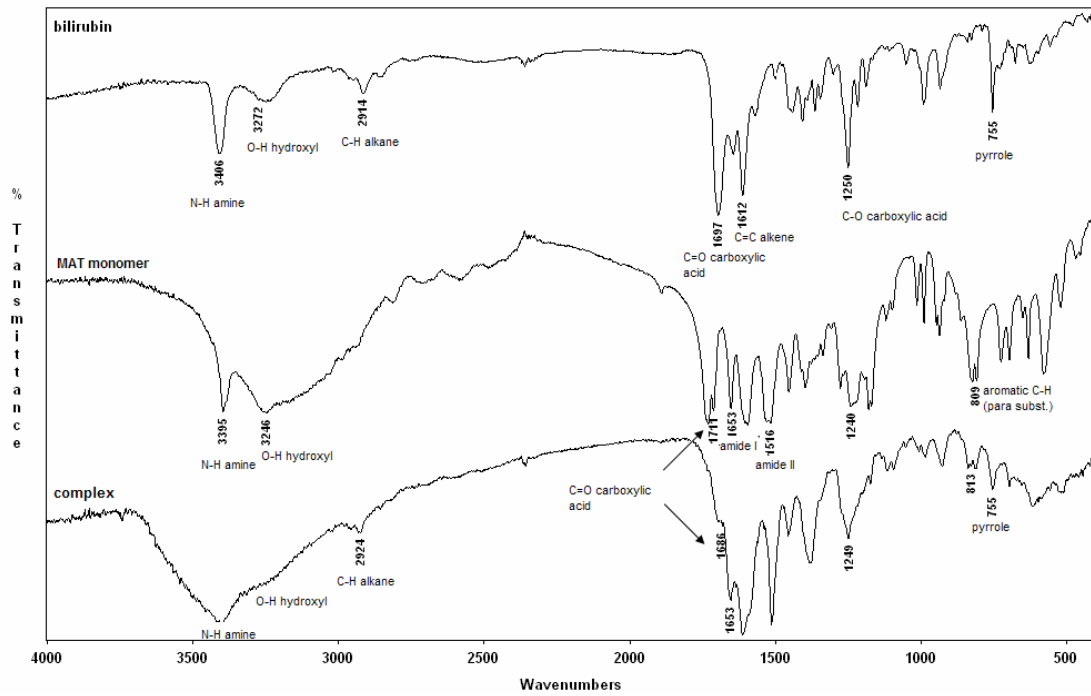


Figure 4.4. FTIR spectra of bilirubin, MAT monomer and MAT-bilirubin complex.

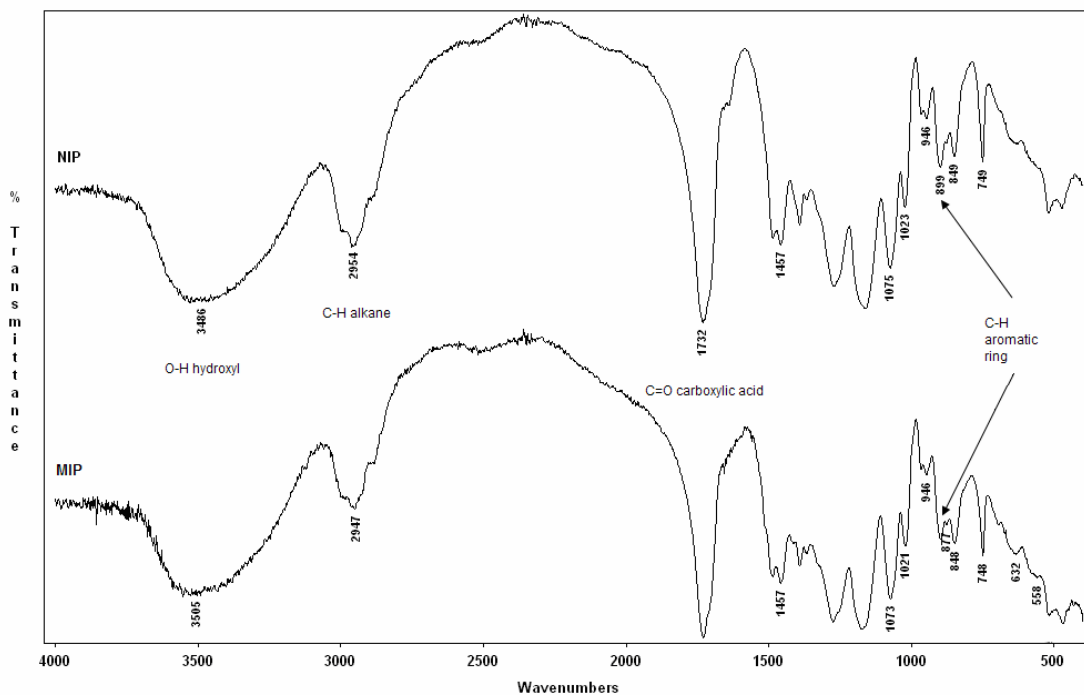


Figure 4.5. FTIR spectra of NIP and MIP particles.



Figure 4.6. Optic Photographs of the synthesized NIP (left) and MIP(right) particles.

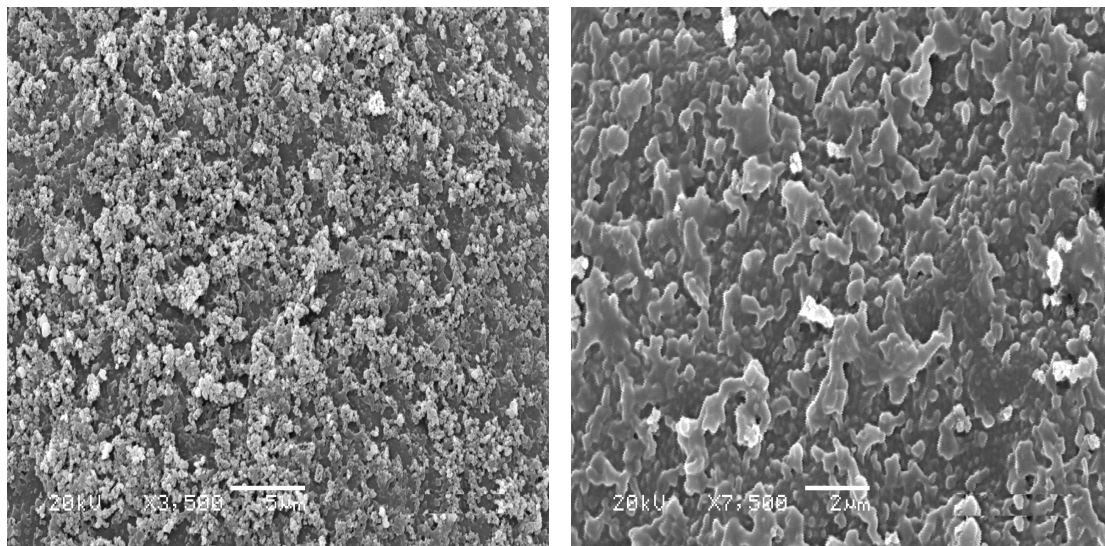
The incorporation of the MAT for MIP and NIP polymers was found to be  $69 \mu\text{mol/g}$  and  $27 \mu\text{mol/g}$  polymer, respectively, by using nitrogen stoichiometry. Note that HEMA and other polymerization ingredients does not contain nitrogen. This nitrogen amount determined by elemental analysis comes from only incorporated MAT groups into the polymeric structure. (N)-methacryloyl-(L)-tyrosine (MAT) was selected as the comonomer and molecularly-imprinted ligand for the selective separation of bilirubin molecules from human plasma.

The bilirubin-imprinted poly(HEMA-MAT) particles are cross linked hydrophilic matrices. The equilibrium swelling ratios of the non-imprinted poly(HEMA-MAT) and bilirubin-imprinted poly(HEMA-MAT) particles used in this study are 51.3% and 64.7%, respectively. The water uptake ratio of the MIP particles increases compared with NIP. Several explanations can be offered. First, formation of molecular cavities in the polymer structure introduces more hydrodynamic volume into the polymer chain, which can adsorb more water molecules into polymer matrices. Second,

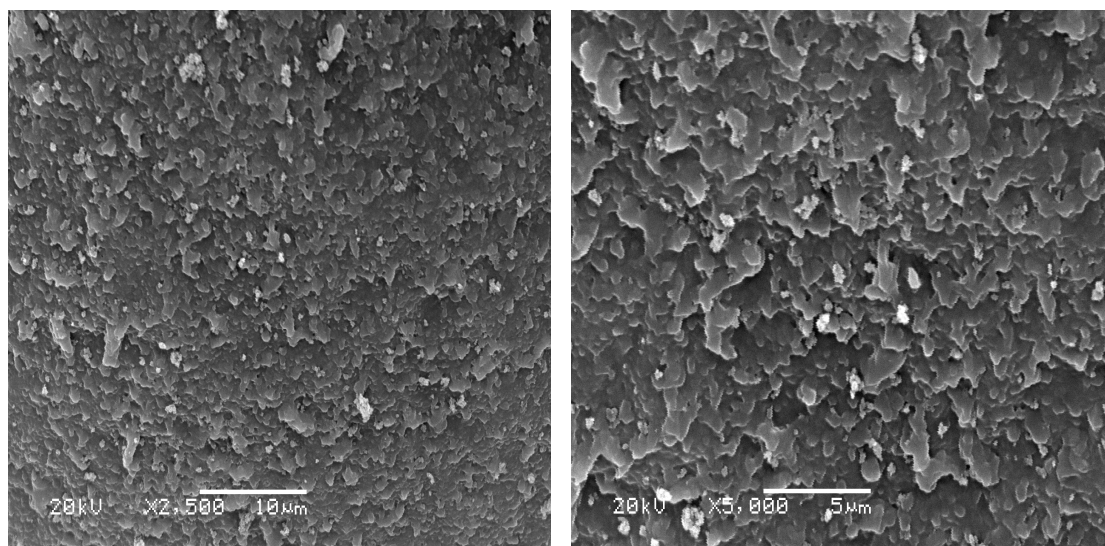
reacting of bilirubin-MAT complex with HEMA effectively increased the length of polymer chains. Therefore, water molecules penetrate into the polymer chains more easily, resulting in an improvement of polymer water uptake in aqueous solutions. It should be noted that these particles are quite rigid, and strong enough due to cross-linked structure. Therefore these imprinted particles are suitable for continuous packed bed applications.

The surface morphology and internal structure of MIP and NIP particles are exemplified by the scanning electron micrographs. The bulk structure of the MIP and NIP particles were observed with a scanning electron microscope (SEM) in Figure 4.7. Figure 4.7. (A) shows the MIP particles. They are composed of small and interconnected globules which form a porous structure. The size of the globules was roughly determined to be in a 0.5-2  $\mu\text{m}$  in range, according to the enlarged SEM photograph; it should be noted that this size is about five-fold less than those of conventional porous particles packed in chromatographic devices. It is clearly seen that the MIP particles have similar porous structure to the corresponding NIP particles (Figure 4.7. A-B). This similarity is important in quality of competitive studies. These large pores reduce diffusional mass transfer resistance and facilitate convective transport because of high specific internal surface area.

Bilirubin-imprinted particles were synthesized by bulk polymerization. The grounded polymers were sieved and the fraction that fall in the size range of 71-100  $\mu\text{m}$  were used throughout the study.



(A)



(B)

Figure 4.7. SEM micrographs of MIP (A) and NIP (B) poly(HEMA- MAT) particles.

## 4.2. Adsorption of Bilirubin from Human Plasma

Adsorption properties, e.g. adsorption capacity and adsorption rate are also important parameters when MIPs are used as adsorbent in separation fields because adsorption capacity reflecting the adsorption ability of adsorbent and adsorption rate illustrating the speed to reach adsorption equilibrium.

Bilirubin was extracted from the MIP particles extensively with 2 M NaOH and 2M Na<sub>2</sub>CO<sub>3</sub> includes EDTA solution for 48 h at room temperature in dark room before bilirubin adsorption studies from human plasma. This procedure was repeated until no bilirubin leakage was detected from the MIP particles. The ratio of bilirubin extracted was 87% that corresponds to 1.48 mg bilirubin per g polymer. Leakage of bilirubin molecules interior of the particles is harder for the diffusion limitations. It needs much more incubation times.

### 4.2.1. Effect of Time

Figure 4.8 shows the time dependence of the adsorption values of bilirubin molecules on bilirubin-imprinted poly(HEMA-MAT) particles. The adsorption rate was relatively fast, the time required to reach equilibrium conditions was about 60 min.

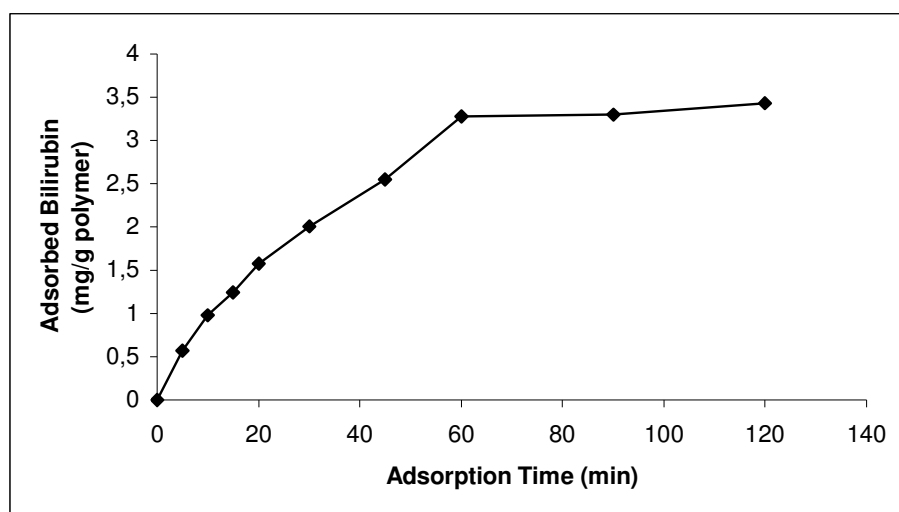


Figure 4.8. Time dependent adsorption of bilirubin molecules on the MIP particles;  $V_{\text{total}}$ ; 10 mL, 0.8 mg/mL solution, 125 mg polymer and T: 25 °C.

The maximum adsorption capacity for bilirubin was 3.41 mg per gram dry weight of particles. This fast adsorption equilibrium is most probably due to high complexation and geometric affinity between bilirubin molecules and bilirubin cavities in the particles structure.

For the extracorporeal removal of bilirubin by various adsorbents, a wide range of adsorption rates have been reported in the literature. For example, Chandy and Sharma considered 2 h as an equilibrium adsorption time in their bilirubin removal studies, in which they used polylysine-immobilized chitosan beads [8]. Morimoto et al have studied bilirubin removal in patients with postoperative hepatic failure on an anion-exchange resin column made of styrene-divinyl benzene and each session lasted a mean of 3 h [10]. Total bilirubin level was drastically reduced to 40% of the perfusion level. Avramescu et al have studied bilirubin adsorption on a column contained ethylene vinyl alcohol polymeric membranes having bovine serum albumin and the adsorption process is completed 6 h [11]. Syu et al. prepared bilirubin imprinted poly(MAA-EGDMA) particles and their adsorption results were determined to be approximately 2 h from which the time to achieve equilibrium adsorption [39]. Xia et al. studied bilirubin removal using Cibacron Blue F3GA attached microporous nylon membrane and reported 10 h adsorption time [39]. Annesini et al. have considered 5 h as a quite fast adsorption time in their bilirubin removal studies, in which they used an anion-exchange styrene-divinyl benzene resin [40]. A patient diagnosed having fulminant hepatitis have been treated using commercial Plasmasorb BR 350 anion exchange column around 1 h effective treatment time [41] for the removal of bilirubin. The flow rate in the aqueous phase, structural properties of adsorbent (e.g. porosity, surface area), amount of adsorbent, adsorbate properties (e.g. molecular dimensions and solubility), initial concentration of bilirubin determine the adsorption rate. In this study, the hyperbilirubinemia patient plasma was incubated MIP particles for 2 h. It can be concluded that the removal rates obtained with the bilirubin imprinted particles used in this study seem to be quite promising.

#### 4.2.2. Effect of Equilibrium Concentration of Bilirubin

Figure 4.9 shows the equilibrium concentration of bilirubin molecules dependence of the adsorbed amount of the bilirubin onto the MIP particles. The adsorption values increased with increasing concentration of bilirubin molecules, and a saturation value is achieved at bilirubin concentration of 0.8 mg/mL, which represents saturation of the active binding cavities on the MIP particles. Maximum adsorption capacity was 3.41 mg/g dry polymer.

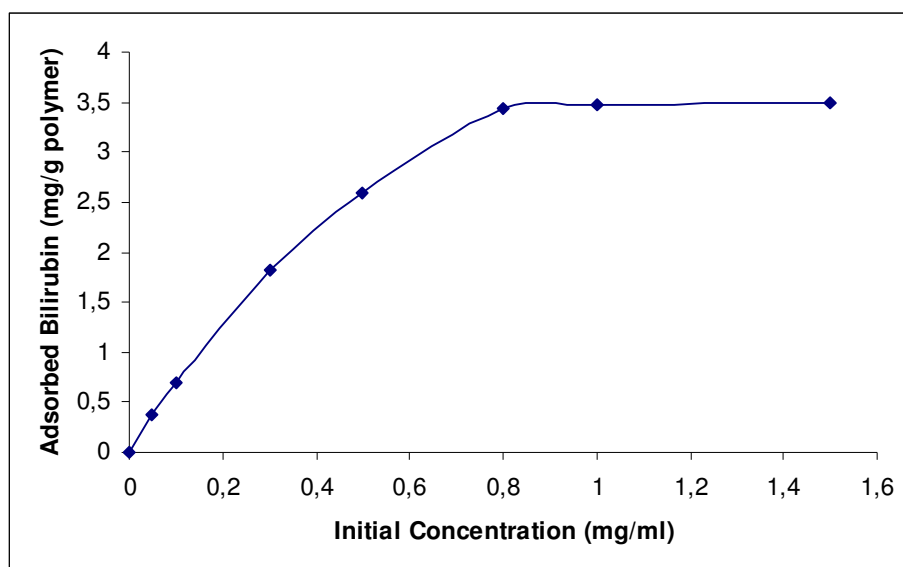


Figure 4.9. Effect of initial bilirubin concentration on adsorption of bilirubin molecules on MIP particles.  $V_{\text{total}}$ : 10 mL ; 125 mg polymer, time: 60 min, T: 25°C.

Recently, research interest focused on preparation of bilirubin adsorbents with reactive ligands including different peptide sequences and dye ligands. A comparison of the adsorption capacity of MIP particles with those of some other affinity adsorbents reported in literature is given in Table 4.1. The adsorption capacity of MIP particles was good when compared with other adsorbents. Differences of bilirubin adsorption capacity are due to the properties of each adsorbent such as structure, functional groups, ligand loading and accessible surface area.

Table 4.1. Comparison of the adsorption capacities for bilirubin of various adsorbents.

Material	Ligand/Interaction type	Adsorption capacity (mg/g)	[R]
Polyacrylamide beads	Poly-L-lysine Poly-D-lysine Poly-L-ornithine	0.2-75	[3]
Macroreticular resin	Albumin	2-24	[5]
Chitosan particles	Poly-L-lysine	1.5	[8]
Poly(glycidyl methacrylate- divinylbenzene copolymer	Albumin	30	[13]
Poly(hydroxyethyl methacrylate) particles	Cibacron Blue F3GA Alkali Blue 6B Congo Red	6.8-32.5	[15-18]
Polyamide hollow fiber	Cibacron Blue F3GA	48.9	[19]
Poly(ethylene vinyl alcohol)	Bovine serum albumin	25.0	[11]
Chitosan coupled nylon membrane	Cibacron Blue F3GA	64.7	[39]
Anion exchange resin	Ion-exchange	4.0-80	[42]
Poly(tetrafluoroethylene) membrane	Cibaron Blue F3GA	76.2	[43]
Polyamide resin	Aminoacid	5-80	[44]
IONEX Polypropylene fiber	Tertiary amine	7.7	[45]
Polyacrylonitrile membrane	Hepatocyte receptor	2.8	[46]
Polybutadiene- hydroxyethyl methacrylate gels	Bovine serum albumin	3.1	[47]
Partially aminated polyacrylamide	$\beta$ -cyclodextrin	42.2	[48]
Poly(hydroxyethyl methacrylate) magnetic particles/batch studies	Human serum albumin	64.7	[49]
Cellulose acetate fiber	Cibaron Blue F3GA	4.0	[50]
Poly(hydroxyethyl methacrylate) magnetic particles/MSFB	Human serum albumin	88.3	[51]
Poly(MAA-EGDMA)/MIP	Molecular recognition	1.04	[52]
Poly(HEMA-MAT)/MIP	Molecular recognition	3.41	in this study

#### 4.2.3. Langmuir Adsorption Model And Adsorption Dynamics

An adsorption isotherm is used to characterize the interactions of each molecule with the adsorbents. This provides a relationship between the concentration of the

molecules in the solution and the amount of protein adsorbed on the solid phase when the two phases are at equilibrium. The Langmuir adsorption model assumes that the molecules are adsorbed at a fixed number of well-defined sites, each of which is capable of holding only one molecule. These sites are also assumed to be energetically equivalent and distant from each other so that there are no interactions between molecules adsorbed on adjacent sites.

During the batch experiments, adsorption isotherms were used to evaluate adsorption properties. The Langmuir adsorption isotherm is expressed by Eq. 4.1. The corresponding transformations of the equilibrium data for bilirubin molecules gave rise to a linear plot, indicating that the Langmuir model could be applied in these systems and described by the equation:

$$Q = Q_{\max} \cdot b \cdot C_{\text{eq}} / (1 + bC_{\text{eq}}) \quad (4.1)$$

where  $Q$  is the concentration of bound bilirubin in the adsorbent (mg/g),  $C_{\text{eq}}$  is the equilibrium bilirubin concentration in solution (mg/g),  $b$  is the Langmuir constant (g/mg) and,  $Q_{\max}$  is the adsorption capacity (mg/g). This equation can be linearized so that

$$C_{\text{eq}} / Q_{\text{eq}} = 1 / (Q_{\max} \cdot b) + (C_{\text{eq}} / Q_{\max}) \quad (4.2)$$

The plot of  $C_{\text{eq}} / Q_{\text{eq}}$  versus  $C_{\text{eq}}$  was employed to generate the intercept of  $1/Q_{\max}$  and the slope of  $1/Q_{\max} \cdot b$  (Figure 4.10).

The maximum adsorption capacity ( $Q_{\max}$ ) data for the adsorption of bilirubin molecule was obtained from the experimental data. The correlation coefficients ( $R^2$ ) were 0.9946. The Langmuir adsorption model can be applied in this affinity adsorbent system. It should be also noted that the maximum adsorption capacities ( $Q_{\max}$ ) and the Langmuir constants were found to be 3.95 mg/g and 8.37 g/mg, respectively.

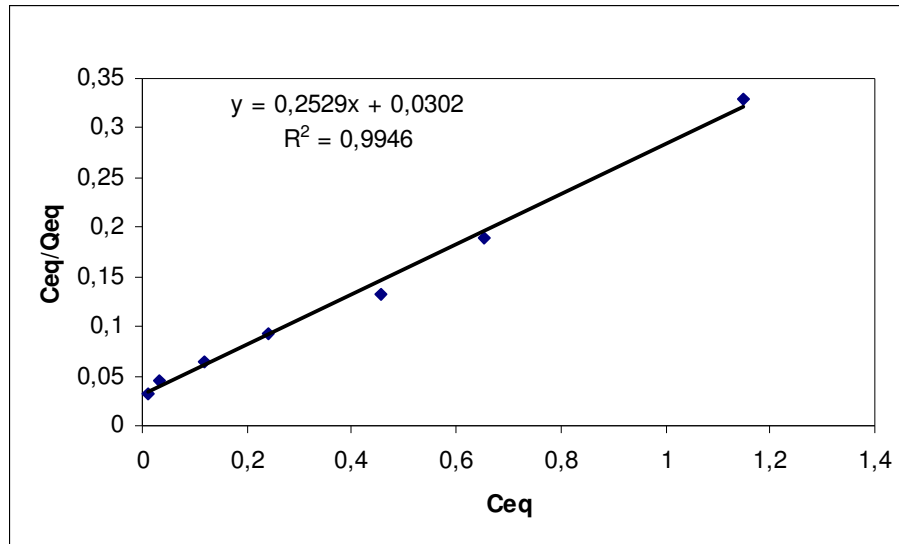


Figure 4.10. Langmuir adsorption isotherm of the MIP particles; T: 25 °C.

The maximum adsorption capacity ( $Q_{\max}$ ) data for the adsorption of bilirubin molecule was obtained from the experimental data. The correlation coefficients ( $R^2$ ) were 0.9946. The Langmuir adsorption model can be applied in this affinity adsorbent system. It should be also noted that the maximum adsorption capacities ( $Q_{\max}$ ) and the Langmuir constants were found to be 3.95 mg/g and 8.37 g/mg, respectively.

The other well-known isotherm, which is frequently used to describe adsorption behavior, is the Freundlich isotherm. This isotherm is another form of the Langmuir approach for adsorption on a heterogeneous surface. The amount of adsorbed molecule is the summation of adsorption on all binding sites. The Freundlich isotherm describes reversible adsorption and is not restricted to the formation of the monolayer. This empirical equation takes the form:

$$Q_{eq} = K_F (C_{eq})^n \quad (4.3)$$

Where,  $K_F$  and  $n$  are the Freundlich constants. This equation can be linearized so that

$$\ln Q_{eq} = \ln K_F + (n \times \ln C_{eq}) \quad (4.4)$$

The plot of  $\ln Q_{eq}$  versus  $\ln C_{eq}$  was employed to generate the intercept of  $\ln K_F$  and the slope of 'n' (Figure 4.11).

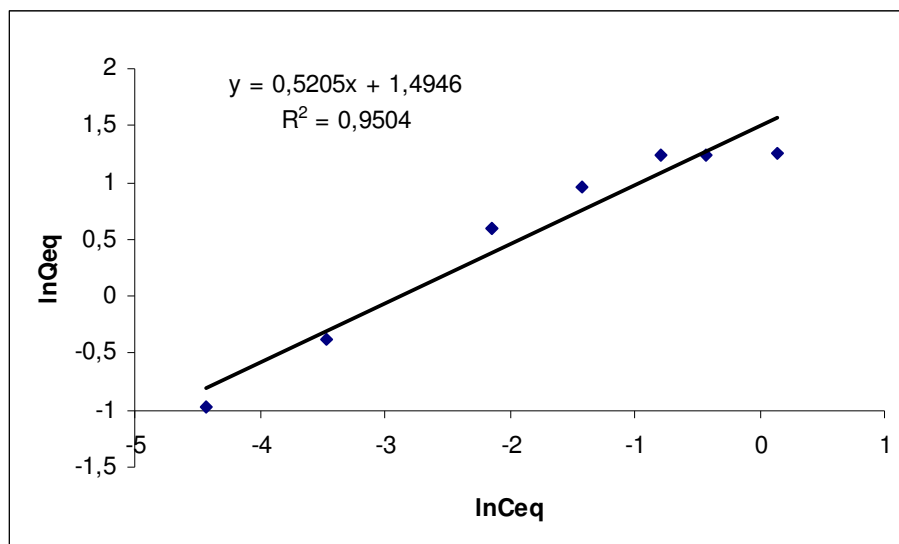


Figure 4.11. Freundlich adsorption isotherm of the MIP particles ; T: 25 °C.

The adsorption isotherms of bilirubin-imprinted poly(HEMA-MAT) were found to be linear over the whole concentration range studies and the correlation coefficients were high (Figure 4.10-4.11). According to the correlation coefficients of isotherms, Langmuir adsorption model is favorable. Table 4.2 summarizes the Langmuir and Freundlich adsorption isotherm constants,  $K_d$ ,  $n$  and  $K_F$  and the correlation coefficients.

Table 4.2. Langmuir and Freundlich adsorption isotherm constants

	Experimental	Langmuir constants			Freundlich constants		
	$Q_{exp}$ (mg/g)	$Q_{max}$ (mg/g)	$K_d$ (g/mg)	$R^2$	$K_F$	$N$	$R^2$
MIP particles	<b>3.41</b>	<b>3.95</b>	<b>8.37</b>	<b>0.9946</b>	<b>4.45</b>	<b>0.52</b>	<b>0.9504</b>

In order to examine the controlling mechanism of adsorption process such as mass transfer and chemical reaction, kinetic models were used to test experimental data. The kinetic models (Pseudo-first and second-order equations) can be used in this case assuming that the measured concentrations are equal to adsorbent surface

concentrations. The first-order rate equation of Lagergren is one of the most widely used for the adsorption of solute from a liquid solution [53]. It may be represented as follows:

$$\Delta q_t/dt = k_1(q_{eq} - q_t) \quad (4.5)$$

where  $k_1$  is the rate constant of pseudo-first order adsorption ( $\text{min}^{-1}$ ) and  $q_{eq}$  and  $q_t$  denote the amounts of adsorbed protein at equilibrium and at time  $t$  (mg/g), respectively. After integration by applying boundary conditions,  $q_t=0$  at  $t=0$  and  $q_t=q_t$  at  $t=t$ , gives

$$\log[q_{eq}/(q_{eq} - q_t)] = (k_1 t)/2.303 \quad (4.6)$$

Equation 4.6 can be rearranged to obtain a linear form

$$\log(q_{eq} - q_t) = \log(q_{eq}) - (k_1 t)/2.303 \quad (4.7)$$

a plot of  $\log(q_{eq})$  versus  $t$  should give a straight line to confirm the applicability of the kinetic model. In a true first-order process  $\log(q_{eq})$  should be equal to the interception point of a plot of  $\log(q_{eq} - q_t)$  via  $t$ .

In addition, a pseudo-second order equation based on adsorption equilibrium capacity may be expressed in the form,

$$\Delta q_t/dt = k_2 (q_{eq} - q_t)^2 \quad (4.8)$$

Where  $k_2$  ( $\text{g mg}^{-1} \text{min}^{-1}$ ) is the rate constant of pseudo-first order adsorption process. Integrating equation 4.8,  $q$  and applying the boundary conditions,  $q_t=0$  at  $t=0$  and  $q_t=q_t$  at  $t=t$ , leads to

$$1/(q_{eq} - q_t) = (1/q_{eq}) + k_2 t \quad (4.9)$$

or equivalently for linear form

$$(t/q_t) = (1/k_2 q_{eq}^2) + (1/q_{eq}) t \quad (4.10)$$

a plot of  $t/q_t$  versus  $t$  should give a linear relationship for the applicability of the second-order kinetics. The rate constant ( $k_2$ ) and adsorption at equilibrium ( $q_{eq}$ ) can be obtained from the intercept and slope, respectively.

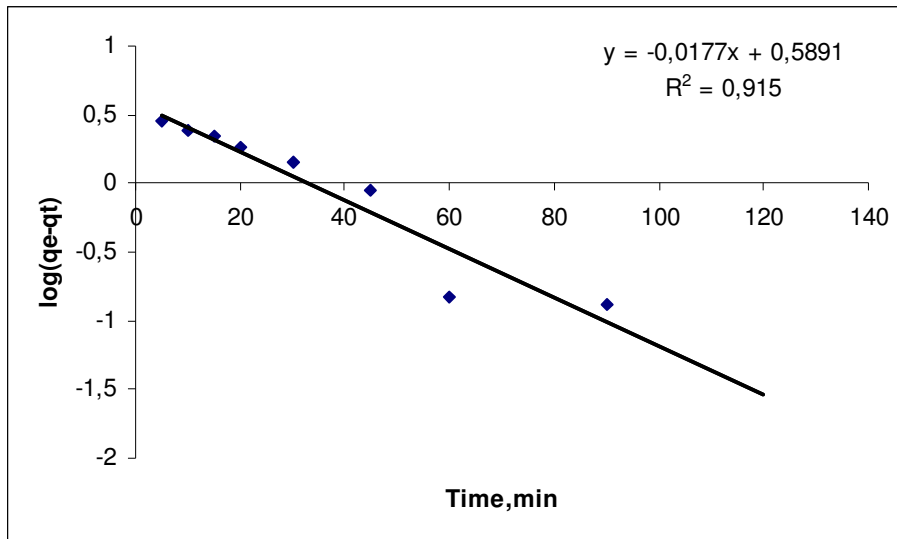


Figure 4.12. Pseudo-first-order kinetic of the experimental data for the adsorbent.

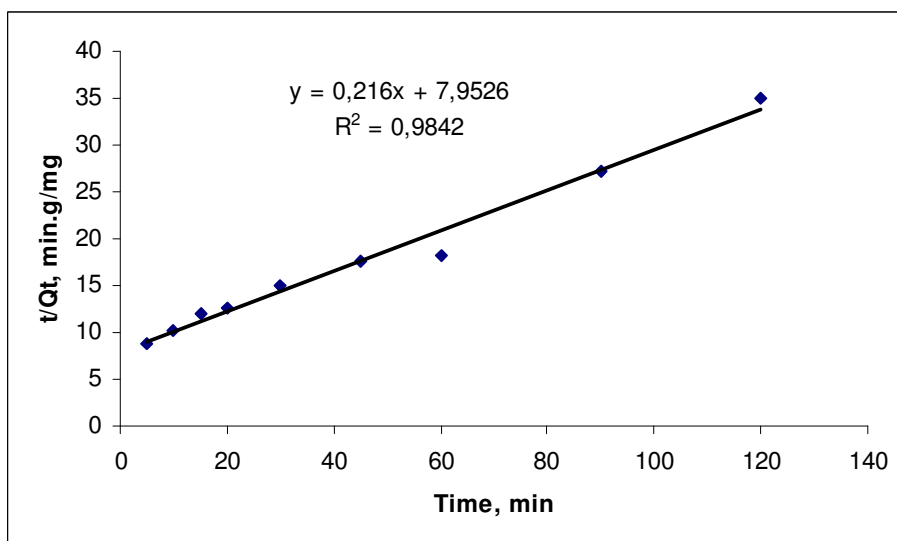


Figure 4.13. Pseudo-second-order kinetic of the experimental data for the adsorbent.

Table 4.3. The first and second order kinetic constants for the MIP particles.

Initial Conc. (mg/mL)	Experimental	First-order kinetic			Second-order kinetic		
		<i>slope</i>	<i>intercept</i>		<i>intercept</i>	<i>Slope</i>	
	Q <sub>eq</sub> (mg/g)	k <sub>1</sub> (1/min)	q <sub>eq</sub> (mg/g)	R <sup>2</sup>	k <sub>2</sub> (g/mg.min)	q <sub>eq</sub> (mg/g)	R <sup>2</sup>
0.8	3.41	0.0414	3.88	0.915	5.87 10 <sup>-3</sup>	4.63	0.984

Table 4.3 shows the results which are for both first order and the second order kinetic models. The results show that the second order mechanism is applicable ( $R^2$  values are the highest). These results suggest that the pseudo-second order mechanisms is predominant and that chemisorption might be the rate-limiting step that controls the adsorption process. The rate-controlling mechanism may vary during the course of the adsorption process three possible mechanisms may be occurring [53]. There is an external surface mass transfer or film diffusion process that controls the early stages of the adsorption process. This may be followed by a reaction or constant rate stage and finally by a diffusion stage where the adsorption process slows down considerably [54].

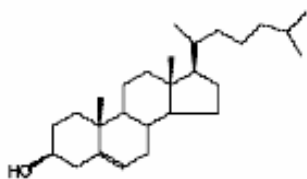
#### 4.2.4. Selectivity Experiments

Molecular recognition selectivity is the most important parameter in characterizing MIPs because molecular recognition is the essential character of MIPs.

Competitive adsorptions of bilirubin/cholesterol and bilirubin/testosterone from their mixtures were also studied in a batch system. Cholesterol and testosterone were chosen as competitive molecules.

Figure 4.14. shows the chemical structures of cholesterol, testosterone and bilirubin, are shown in Figure 4.14. (a-b-c), respectively. Molecular weight of bilirubin is 584 g/mol while that of cholesterol is 386 g/mol and that of testosterone is 288 g/mol. Their molecular weights indicate that these molecules are of a similar size.

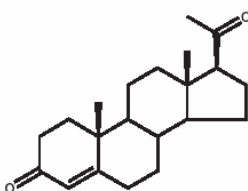
Cholesterol and testosterone were chosen for the comparison because they, together with bilirubin, are always found in the serum. Hence, to know how they interfere binding of bilirubin by the MIP is essential for the in vitro measurement of serum samples.



Cholesterol

Mw:386 g/mol

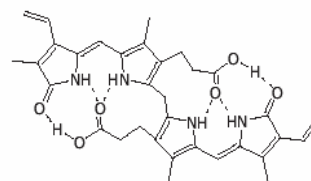
(a)



Testosterone

Mw:288 g/mol

(b)



Bilirubin

Mw:584 g/mol

(c)

Figure 4.14. Chemical structures of competitive molecules.

Table 4.4.  $K_d$ ,  $k$ , and  $k'$  values of cholesterol and testosterone with respect to bilirubin.

Molecules	NIP Particles		MIP Particles		
	$K_d$ (mL/g)	K	$K_d$	k	$K'$
Bilirubin	1.36	-	5.00	-	-
Cholesterol	0.53	2.56	0.31	16.18	6.32
Testosterone	0.23	5.91	0.28	17.86	3.02

A comparison of the  $K_d$  values for the MIP samples with the control samples shows an increase in  $K_d$  for bilirubin while  $K_d$  decrease for cholesterol and testosterone. The relative selectivity coefficient is an indicator to express protein adsorption affinity of recognition sites to the imprinted bilirubin molecules. These results show that relative selectivity coefficients of imprinted particles for bilirubin/cholesterol and bilirubin/testosterone were 6.32 and 3.02 times greater than non-imprinted matrix, respectively. Cholesterol and testosterone were less adsorbed by the MIP because of their fewer chances to form hydrogen bonds compared to bilirubin. Nevertheless, the binding specificity for bilirubin from imprinted poly (HEMA-MAT) was sufficient for the

recognition of bilirubin from other compounds. Table 4.4. summarizes the  $K_d$ ,  $k$  and  $k'$  values in selectivity studies. Figure 4.15 shows the adsorbed template and competitive molecules both in MIP and NIP particles in mg/g polymer.

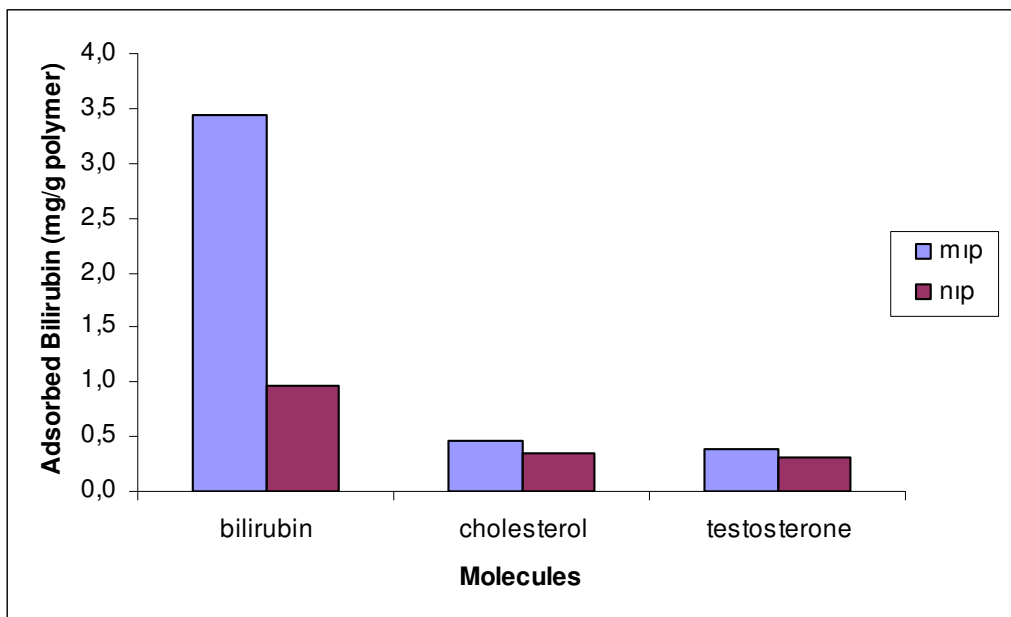


Figure 4.15. Adsorbed template and competitive molecules both in MIP and NIP particles. 0.8 mg/mL, 10 mL solution, 125 mg polymer, T:25 °C.

### 4.3. Desorption and Repeated Use

In order to show the stability and reusability of the MIP particles, the adsorption-desorption cycle was repeated five times using the same polymeric particles in a batch experimental set-up. For sterilization after one adsorption-desorption cycle, the particles were washed with 50 mM NaOH solution for 30 min. After this procedure, particles were washed with distilled water for 30 minutes. At the end of five adsorption-desorption cycle, there was no remarkable decrease in the adsorption capacity (Figure 4.16). As seen in here that the polymer beads are very stable, and maintain their adsorption capacity at almost constant value of 87%.

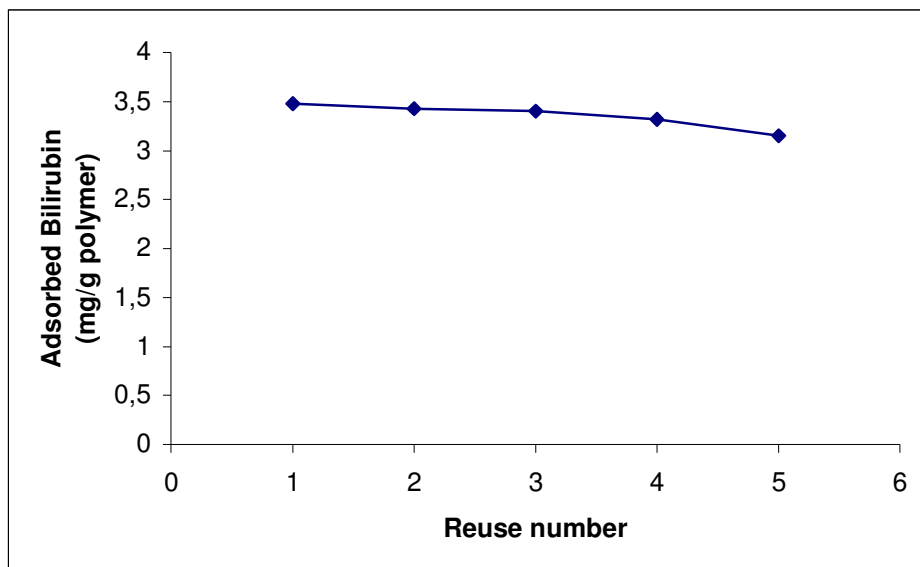


Figure 4.16. Adsorption-desorption cycle of MIP particles.  $V_{\text{total}}$ : 10 mL ; 125 mg polymer, time: 30 min, T: 25°C.

## 5. CONCLUSION

- The bulk polymerization procedure provided cross-linked bilirubin imprinted p(HEMA-MAT) particles.
- The equilibrium swelling ratios of the NIP and MIP particles used in this study, which were prepared with the recipe given in section 4.1 are 51,3% and 64,7%, respectively.
- Due to the elemental analysis results, NIP and MIP particles have approximately 69  $\mu\text{mol/g}$  and 27 $\mu\text{mol/g}$  MAT content respectively.
- The MIP particles has an homogeneous appearance with regularly-shaped and sphere-like small nodules. The size of the globules was roughly determined to be in a 0.5-2  $\mu\text{m}$  range, according to an enlarged SEM photograph.
- The adsorption rate was relatively very fast, the time required to reach equilibrium conditions was about 60 min. The maximum adsorption capacity for bilirubin molecules was 3,41 mg per gram dry weight of particles. This fast adsorption equilibrium is most probably due to high complexation and geometric affinity between bilirubin molecules and bilirubin cavities in the particle structure.
- The adsorption values increased with increasing concentration of bilirubin, and a saturation value is achieved at protein concentration of 0,8 mg/mL, which represents saturation of the active binding cavities on the MIP poly(HEMA-MAT) particles.
- The maximum adsorption capacity ( $Q_{\text{max}}$ ) data for the adsorption of bilirubin molecules was obtained from the experimental data. The correlation coefficients ( $R^2$ ) were 0,9946. The Langmuir adsorption model can be applied in this affinity adsorbent system. It should be also noted that the maximum adsorption

capacities ( $Q_{max}$ ) and the Langmuir constants were found to be 3.95 mg/g and 0.9946 respectively.

- A comparison of the  $K_d$  values for the bilirubin imprinted poly(HEMA-MAT) samples with the control samples shows an increase in  $K_d$  for bilirubin while  $K_d$  decrease for cholesterol and testosterone.
- The desorption time was found to be 2 hour. Desorption ratios are high (up to 87%). The adsorption capacity of the recycled the bilirubin-imprinted poly(HEMA-MAT) particles can still be maintained at 90% level at the 5th cycle. The MIP poly(HEMA-MAT) particles can be used many times without decreasing their adsorption capacities significantly.

## 6. REFERENCES

1. K.H. Lee, J. Wendon, M. Lee, M.D. Costa, S.G. Lim, K.C. Tan, *Liver Transplantation*, 8 (2002) 591.
2. C. Tiribelli, J.D. Ostrow, *J. Hepatology*, 43 (2005) 156.
3. X.X. Zhu, G.R. Brown and L.E. St-Pierre, *Biomat. Artif. Cells, Artif. Organs*, 18 (1990) 75.
4. C.X. Xu, X.J. Tang, Z. Niu and Z.M. Li, *Int. J. Artif. Organs*, 4 (1981) 200.
5. S. Sideman, L. Mor, D. Mordohovich, M. Mihich, O. Zinder and J.M. Brandes, *Trans. Am. Soc. Artif. Intern. Organs*, 27 (1981) 434.
6. Y. Idezuki, M. Hamaguchi, S. Hamabe, H. Moriya, T. Nagashima, H. Watanabe, T. Sonoda, K. Teramoto, T. Kikuchi and H. Tanzawa, *Trans Am Soc Artif Intern Organs*, 27 (1981) 428.
7. G.R. Brown, *Int. J. Biochromatogr.*, 1 (1994) 73.
8. T. Chandy, and C.P. Sharma, *Artif. Organs*, 16 (1992) 568.
9. Z. Yamazaki, N. Inoue, T. Wada, T. Oda, K. Atsumi, K. Kataoka and Y. Fujisaki, *Trans. Am. Soc. Artif. Intern. Organs*, 25 (1979) 480.
10. T. Morimoto, M. Matsushima, N. Sowa, K. Ide and S. Sawanishi, *Artif. Organs*, 13 (1989) 447.
11. M.E. Avramescu, W.F.C. Sager, Z. Borneman, M. Wessling, *J. Chromatogr. B.*, 803 (2004) 215.
12. Y. Yu, B. He, H. Gu, *Artif. Cells Blood Subs. Immob. Biotech.*, 28 (2000) 307.
13. H. Kuroda, T. Ranaka, Z. Osawa, *Die Angewadte Makromolekulare Chemie*, 237 (1996) 143.
14. N. Ahmad, K. Arif, S.M. Faisal, M.K. Neyaz, S. Tayyab, M. Owais, *Biochim. Biophys. Acta*, 1760 (2006) 227.
15. M. Kocakulak, A. Denizli, A.Y. Rad, E. Piflkin, *J. Chromatogr B*, 693 (1997) 271.
16. A. Denizli, M. Kocakulak, E. Piflkin, *J. Macromol. Sci., Pure & Appl. Chem.*, A35 (1998) 137.
17. A. Denizli, M. Kocakulak, E. Pişkin, E., *J. Appl. Polym. Sci.*, 68 (1998) 373.
18. A. Denizli, M. Kocakulak, E. Pişkin, E., *J. Chromatogr B*, 707 (1998) 25.
19. S. fienel, F. Denizli, H. Yavuz, A. Denizli, *Sep. Sci. Technol.*, 37 (2002) 1989.
20. K. Mosbach, *Trends Polym Sci* 34 (1994) 1812.
21. B. Sellergren (Ed), *Molecularly imprinted polymers: man-made mimics of antibodies*

- and their application in analytical chemistry. Elsevier, Amsterdam (2001).
22. G. Wulff and K. Knorr, *Bioseparation* 10 (2002) 257.
  23. M. Whitcombe, M.E. Rodriguez, P. Villar, E.N. Vulfon, *J. Am. Chem. Soc.* 117 (1995) 7105.
  24. M. Andac, R. Say, A. Denizli, *J. Chromatogr. B.*, 811 (2004) 119.
  25. M. Andac, E. Ozyapı, S. Senel, R. Say, A. Denizli, *Ind. Eng. Chem. Res.*, 45 (2006) 1780.
  26. S.C. Zimmerman and N.G. Lemcoff, *Chem Commun* 1 (2004) 5.
  27. Q. Fu, H. Sanbe, C. Kagawa, K.K. Kunitomo and J. Haginaka, *Anal Chem* 75 (2003) 191.
  28. S. Büyüktiryaki, R. Say, A. Ersöz, E. Birlik, A. Denizli, A., *Talanta*, 67 (2005) 640.
  29. H. Shi, W.B. Tsai, M.D. Garrison, S. Ferrari and B.D. Ratner, *Nature* 398 (1999) 593.
  30. M.J. Syu, J.H. Deng, Y.M. Nian, *Anal. Chim. Acta*, 504 (2004) 167.
  31. M.J. Syu, Y.M. Nian, *Anal. Chim. Acta*, 539 (2005) 97.
  32. M.J. Syu, J.H. Deng, Y.M. Nian, T.C. Chiu, A.H. Wu, *Biomaterials*, 26 (2005) 4684.
  33. M.J. Syu, A. H.Wu, *Biosensors Bioelectronics* 2005 (in press)
  34. G.R. Buettner, D.L. W. Oberley. *Free Radicals in Biology and Medicine* (2001) 77:222
  35. J.S. Ultman, L. Xiong, 2006, A Review Paper, Pennsylvania State University
  36. M. Odabaşı, *Molecularly Imprinted Polymers For Separation Of Proteins*, A thesis of PhD, Hacettepe University, Natural and Applied Sciences, Ankara
  37. S. Özkara Yavuz, *Ion-Selective Imprinted Monolithic Columns For Iron Removal From Human Serum Plasma*, A thesis of PhD, Hacettepe University, Natural and Applied Sciences, Ankara
  38. A. Müge Andaç, *Ion-Selective Imprinted Polymer Beads For Metal Detoxification From Human Plasma* A thesis of MsC, Hacettepe University, Natural and Applied Sciences, Ankara
  39. B. Xia, G. Zhang, F. Zhang, *J. Membr. Sci.*, 226 (2003) 9.
  40. M.C. Annesini, L. Di Paola, L. Marrelli, V. Piemonte, L. Turchetti, *Int. J. Artif. Organs*, 28 (2005) 686.
  41. H. Ishida, S. Sato, A. Sannomiya, K. Tsuji, *Transplantation Proceedings*, 32 (2000) 2241.
  42. C.R. Davies, P.S. Malchesky and G.M. Saide, *Artif Organs*, 14 (1990) 14.

43. L. Zhang, G. Jin, *J. Chromatogr. B.*, 821 (2005) 112.
44. D.S. Henning, G.R. Brown and L.E. St-Pierre, *Int. J. Artif. Organs*, 9 (1986) 33.
45. F. Kanai, T. Takahama, I. Iizuka, M. Hiraishi, Z. Yamazaki, Y. Fujimori, Y. Maruyama, T. Wada, K. Asano, T. Sonoda, *Artificial Organs*, 9 (1985) 75.
46. I.A. Chernova, K.Y. Gurevich, *J. Membr. Sci.*, 113 (1996) 161.
47. C. Alvarez, M. Strumia, H. Bertorello, *J. Biochem. Biophys. Methods*, 49 (2001) 649.
48. H. Wang, J. Ma, Y. Zhang, B. He, *React. Funct. Polym.*, 32 (1997) 1.
49. A.Y. Rad, H. Yavuz, M. Kocakulak, A. Denizli, *Macromol. Biosci.*, 3 (2003) 471.
50. Z. Ma, M. Kotaki, S. Ramakrishna, *J. Membr. Sci.*, 265 (2004) 155.
51. L. Uzun, A. Denizli, *J. Biomater. Sci. Polym. Ed.*, 17 (2006) 791.
52. Y.S. Ho, G. McKay, *Proc. Biochem.*, 34 (1999) 451.
53. S. Oncel, L. Uzun, B. Garipcan, A. Denizli, *Ind. Eng. Chem. Res.*, 44 (2005) 7049.
54. S.J. Allen, B. Koumanova, Z. Kircheva, S. Nenkova, *Ind. Eng. Chem. Res.*, 44 (2005) 2281.

**CIRRUCULUM VITAE**

Name : Gözde  
Surname : Baydemir  
Date of Birth : 26.01.1980  
Place of Birth : Adana, Turkey  
Gender : Female  
Nationality : Turkish  
Marital Status : Single  
Foreign Language : English  
Mail Address : Hacettepe University, Chemistry Department, Beytepe, 06532  
Ankara, TURKEY  
Telephone : (+90 312) 297 79 63  
Fax : (+90 312) 299 21 63  
e-mail : [gbaydemir@hacettepe.edu.tr](mailto:gbaydemir@hacettepe.edu.tr)

**EDUCATION**

BSc Chemistry Department, Hacettepe University, Ankara, 1999-2003

MSc Chemistry Department, Biochemistry Div., Hacettepe University, Ankara, 2003-2006